Chloride exchanges between oceanic sediments and seawater: constraints from chlorine isotopes

Pierre Agrinier, Joris Gieskes, Gowtham Subbarao, Gerard Bardoux, Magali Bonifacie

Chloride exchanges between oceanic sediments and seawater: constraints from chlorine isotopes

Pierre Agrinier[1], Joris Gieskes[2], Gowtham Subbarao[2], Gerard Bardoux[1], Magali Bonifacie[1]

[1] Université Paris Cité, Institut de physique du globe de Paris, CNRS, F-75005 Paris, France

[2] Scripps Institution of Oceanography, San Diego, La Jolla, CA, USA

Keywords : chloride, isotopes, pore fluids, oceanic sediments

Abstract

We investigate the chlorine isotope disequilibrium between chlorides in pore fluids and chlorides in seawater and infer its consequences for chlorine isotope exchange between ocean sediment pore fluids and seawater. We illustrate our methodology with pore fluids from two IODP drilled to depths of ≈ 1000 m (U1456 and U1457) in the Indus River fan dominated by clay-detritus sediments of the western Himalayas. At these two sites, the concentrations of chloride and sodium ions do not show significant changes with depth and remain very close to those of seawater. As a function of depth, however, chlorides show a progressive decrease in ^{37}Cl (downto -2.5 and -1.4 ‰ respectively), while Ca^{2+} increases and Mg^{2+} decreases, as commonly observed in clay-rich oceanic sediments. The rate of the $\delta^{37}Cl$ decrease is correlated to the lithology and sedimentation rate. Examining the chlorine budget on these two sites, we conclude that : 1) Most of the chlorine (≥ 96% of the total Cl) is contained in the pore fluids as chlorides, while the chlorine stored in the other sinks (minerals or organochlorine) is generally very minor (representing less than 4% of the total Cl). 2) These other sinks are too small to sequester the lost ^{37}Cl-enriched chlorine, which could compensate for the decreased $\delta^{37}Cl$ of the chlorides observed in the pore fluids (assuming that the pore fluids originally had chlorides

with the chlorine isotopic composition of seawater, $\delta^{37}Cl$ = 0 ‰). (3) This lost ^{37}Cl-enriched chlorine has been released from the sediment into the overlying seawater, with fluxes of about 20 moles of chloride per square metre per kiloyear.

In order to evaluate the consequence of this unbalanced on a global scale, we extend this chlorine budget analysis to 22 other oceanic sites drilled by IODP in a variety of tectonic environments. It is estimated that worldwide oceanic sediment pore fluids contain 1 x 10^{20} moles of chloride with mean $\delta^{37}Cl$ at -2.3 ± 0.1 ‰ and mean chlorinity at 0.290 ± 0.055 mole Cl^- per kg of sediment. Most of the calculated values of the lost ^{37}Cl-enriched chlorine flux are between 3.5 and 45.6 moles of chloride per square metre per kiloyear (mean value of 18.3 mole $Cl.m^{-2}.kyr^{-1}$), corresponding to a typical chloride exchange time between sediments and seawater of between 5.5 and 71 Myr with a mean value of 14 Myr. Importantly, in oceanic sediments, a relationship between the $\delta^{37}Cl$ of the chlorides in their pore fluids and the nature of the detrital minerals (smectite, illite, kaolinite, carbonate, quartz, ...) may exists. This relationship should be modulated by the detrital input from the continents to the oceanic sediments and should therefore be a consequence of the climatic conditions on the continents (mainly rain, temperature). The $\delta^{37}Cl$ of the seawater should vary according to these detrital inputs. The expected range of variation would be between -0.3 to +0.3 ‰. This is consistent with the range of $\delta^{37}Cl$ in seawater predicted by the study of evaporites deposited since 2 Ga (Eggenkamp et al., 2019).

I) Introduction

The budget of terrestrial chloride is important for constraining the stability of the Earth chlorine cycle and, in particular, the history of the ocean salinity – a factor influencing the evolution of life during the Earth's history. Despite this importance, the chloride budget in the Earth's surface domains (seawater, sediments, crust) is still poorly known. The present day

amount of chloride in seawater is well known, but those in other surface reservoirs (oceanic sediments, continental basins and silicate crusts) and the exchanges of chloride between them are less well constrained. The chlorine stable isotopes (^{35}Cl & ^{37}Cl) of chloride have the potential to provide additional constraints on the Earth's surface chloride budget by characterizing oceanic crust (e.g., Bonifacie et al., 2005, 2008a and 2008b, Barnes et al., 2008 and 2009), halite deposits (e.g., Eggenkamp et al., 2015 and 2019), or oceanic sediment pore fluids (e.g., Ransom et al., 1995, Hesse et al., 2000, Spivack et al., 2002, Deyhle et al., 2003, Godon et al., 2004a, Bonifacie et al., 2007, Wei et al., 2008, Agrinier et al., 2019 and 2021). These studies revealed a systematic ^{37}Cl depletion of chlorides compared to seawater chlorides. This depletion was unexpected since these interstitial fluids were originally seawater trapped at the seawater-sediment interface.

To explain these depletions in ^{37}Cl in pore fluids, suggestions have been made, ranging from external causes: the upward advection of ^{37}Cl-depleted fluid into the sediments from greater depths (Ransom et al., 1995; Spivack et al., 2002; Hesse et al., 2006; Wei et al., 2008), to internal cause: the generation of ^{37}Cl-depletion by ion filtration of chlorides when pore fluids are transported through clays during the compaction of the sediments (Godon et al., 2004a; Bonifacie et al., 2007; Agrinier et al., 2019 & 2021, see an ilustration of the ion filtration process in Figure 1 of Agrinier et al. 2021). Based on the fact that these ^{37}Cl depletions have been ubiquitously observed in a large variety of investigated tectonic contexts (proto-oceanic basins, oceanic plateaus, continental margins, ridge flanks, prisms of subduction zones, fluvial fans) Agrinier et al., (2021) concluded that these ^{37}Cl depletions were inherited from an internal process. Agrinier et al. (2019 & 2021) calculated the fractionation of chlorine isotopes of chlorides of pore fluids which could be caused by the ion filtration due to the repulsion of chloride by the negatively charged surface of clays (Phillips and Bentley, 1987). We suggested that the mineralogical nature of the sediment would be the primary factor controlling the

76 importance of the chlorine isotope fractionation in pore fluid chlorides. Smectite which has
77 high charge surface density, would be associated with higher isotope fractionation than illite-
78 chlorite, which has lower charge density or kaolinite, which has an even lower charge density.
79 Carbonate and quartz with quasi-zero charge surface density would not produce chlorine
80 isotope fractionation in chlorides.

81 In the light of this knowledge, we designed the present study with three main objectives: 1)
82 to test the relationship between sediment mineralogy and ^{37}Cl depletion of chlorides in pore
83 fluids from Sites U1456 and U1457, 2) to examine in detail, for these two sites, chloride
84 reservoirs where missing ^{37}Cl-enriched chlorides from the pore fluids could be stored and to
85 establish the chloride budget in sediments , and 3) to extend this chloride budget approach to a
86 large number of oceanic sedimentary piles from different tectonic settings.

87 In relation to the first objective, constraints are provided by the study of young, thick
88 continental terrigenous clastic sediments from the Indus fan drilled at the western margin of
89 the Indian subcontinent during IODP expedition 355 at sites U1456 and U1457 (Pandey et al.,
90 2016a,b & c). These sediments were deposited with high rates of sedimentation, mass
91 transports (sands, turbidites, conglomerates and breccia) that produced complex histories of
92 sedimentation including hiatuses. Their mineralogy is dominated by detrital minerals (quartz,
93 chlorite, illite, feldspar, calcite) with minor clays of detrital origin (Cai et al., 2020; Carter et al.,
94 2020). A priori, these sedimentary characteristics are not favorable to the production and the
95 retention of large ^{37}Cl-depletion (ie., very negative $\delta^{37}Cl$) in pore fluid chlorides due to i) the
96 low abundance of clays with high charge surface density (smectite) and ii) the high abundance
97 of detrital mainly silt-sized grains and sand beds with high permeability sediments, where
98 external fluids might have circulated after the deposition of the sediment.

99 For the second objective, it is necessary to establish chlorine budget equations (including
100 isotopes) and review the chlorine isotope fractionations between chloride of the pore fluids

and chlorine in the other sinks that can store chlorine. This is necessary to estimate the amount of missing ^{37}Cl required to balance the ^{37}Cl depletion of the pore fluid chlorides.

Finally, the third objective is to study the chlorine budgets of a set of 24 sedimentary piles (Ocean Drilling Sites) drilled from a wide range of tectonic contexts (proto-oceanic basins, oceanic plateaus, continental margins, ridge flanks, prisms of subduction zones, fluvial fans, ...) where chlorine isotope data in pore fluids exist. This will lead to a calculation of the amount of ^{37}Cl missing in ocean sediments and deduce the consequences for chloride exchange between ocean sediments and seawater.

II) Lithostratigraphy of the U1456 and U1457 sedimentary piles

Sites U1456 and U1457 of IODP Leg 355, were drilled in close proximity (within ~ 100 km) in the Laxmi Basin of the eastern Arabian Sea. They document mainly the Indus River and Deccan trap detritus and recent (≤ 13 Ma) erosion of the high-relief topography of the western Himalaya, the Tibetan Plateau. In both sedimentary piles, detrital quartz, chlorite, illite, feldspar, and calcite are the main components. Clays (< 2μm, smectite, illite, chlorite, kaolinite) are minor constituents (Pandey et al., 2016b & c; Cai et al., 2020; Khim et al., 2018; Andò et al., 2020; Routledge et al., 2020; Chen et al., 2019 & 2020; Kumar et al., 2019; Clift et al., 2020; Carter et al., 2020). A summary of the main characters is given below:

II.1 Sediments at Sites U1456: Unit I (0 - 121 mbsf) is composed of hemipelagic carbonate ooze and clay with intercalated silty-sandy turbidites. Unit II (121 - 361 mbsf) consists of thick-bedded sandy turbidites with intercalated silty and nannofossil-rich clay layers. Unit III (361 – 731 mbsf) is composed of alternating silty-sandy turbidites, carbonate ooze, and clays. Unit IV (731 - 1100 mbsf) consists of mass wasting deposits, including mainly clay with minor

carbonate breccia in the middle-upper part and carbonate breccia in the lower part (Figure 1).

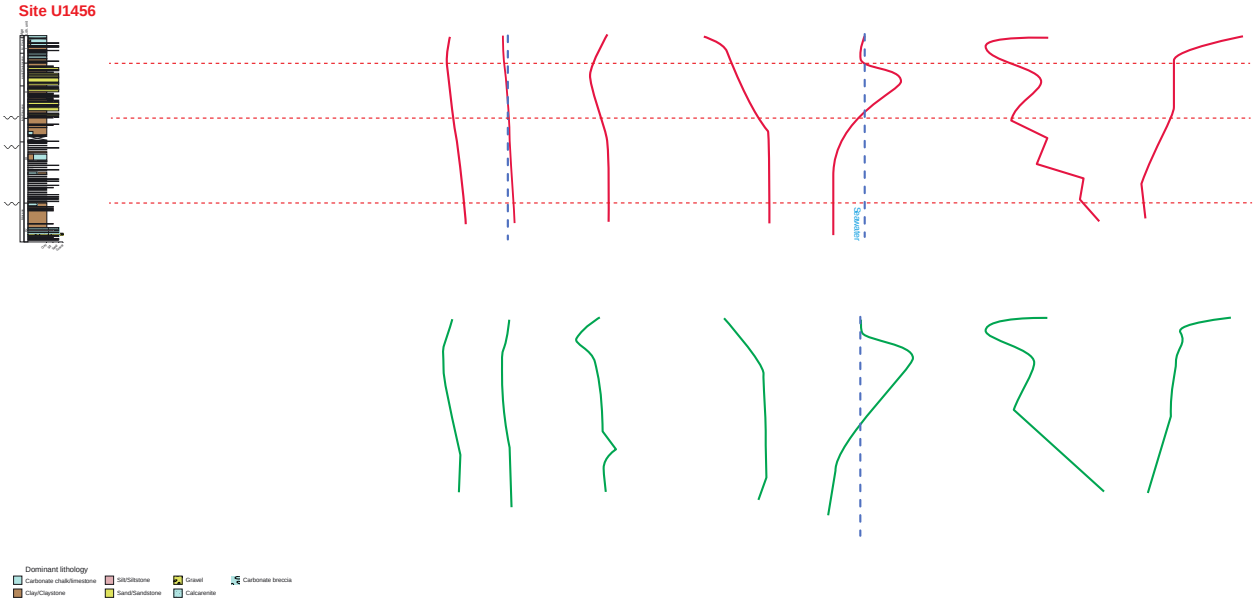

Figure 1: *Sites U1456 and U1457 drilled during IODP Leg 355. From left to right, summary of the lithostratigraphy and profiles of sedimentation rate, porosity, sodium and chloride concentrations, Sodium to chloride and bromide to chloride concentration ratios, Strontium isotope ratio, calcium and magnesium concentrations. All the data are from Pandey et al. (2016b and c) except the Strontium data which are from Carter et al. (2017). Horizontal dashed lines delimit the lithostratigraphic units (I, II, III & IV). Sedimentation rates are computed from the data of Routledge et al. (2020). U1456 porosity data, Φ, are fitted with compaction law $\Phi \approx 75 * exp(-z/400)$ in Unit I ($z \leq 120$ mbsf) and with compaction law $\Phi \approx 48 * exp(-z/5500)$ in Units II, III & IV ($z > 120$ mbsf). U1457 porosity data, Φ, are well fitted with compaction law $\Phi \approx 75 * exp(-z/250)$ in Unit I ($z < 100$ mbsf) and with compaction law $\Phi \approx 50 * exp(-z/3000)$ in Units II & III ($z > 100$ mbsf. The sedimentation rates are not corrected for compaction.*

Sedimentation rates correlate with the nature of the sediments. High rates (410 m/Myr) are obtained for Unit II where mass transport deposits are common. Lower rates are obtained for Units I & III (130 & 60 m/Myr respectively) where mass transport deposits are much less common. The porosity profile correlates with the nature of the sediments. Porosity in Unit I decreases rapidly from 80% at the seawater-sediment interface to 45 % at 121 mbsf, consistent with a high rate of compaction ($\Phi \approx 75 * exp(-z/400)$, Φ : porosity in %, z : depth in meter). In

Units II, III & IV (below 121 mbsf), porosity continues to decrease to ~35% at ~925 mbsf consistent with compaction at a slower rate ($\Phi \approx 48 * \exp(-z/5500)$).

Carbonate abundance is generally below 20 wt.% except at the top of Unit I (0 - 100 mbsf) and at the bottom of Unit IV (below 978 mbsf). XRD clay mineralogy by Cai et al. (2020) shows that in Units I, smectite (≈ 60 %) is the primary clay component with Illite (≈ 30 %). In unit II, Illite (≈ 60 %) dominates the clay fraction, smectite is at ≈ 20 %. In Unit III, at the top, smectite (≈ 60 %) is the primary clay component with Illite (≈ 30 %), while at the bottom, Illite (≈ 60 %) dominates clay fraction, smectite is at ≈ 20 %. Chlorite and Kaolinite are always minor (≤ 10 %).

II.2 Sediments at Site U1457: They are similar to those of Site U1456: Unit I (0 - 74 mbsf) consists of hemipelagic carbonate ooze and clay with intercalated silty-sandy turbidites. Unit II (74 – 385 mbsf) consists of silty clay/claystone intercalated with numerous silty sand beds. Unit III (385 – 835 mbsf) consists of chalk and claystone intercalated with silty sandstone (385 – 835 mbsf). Unit IV (835 – 1062 mbsf) consists of claystone, intercalated with siltstone and carbonate breccia. Sedimentation rates correlate with the nature of the sediments. High rates (600 m/Myr) are obtained for Unit II where mass transport deposits are common. Smaller rates are obtained for Units I & III (70 & 40 m/Myr respectively) where mass transport deposits much less common. Similarly, the porosity profile correlates with the nature of the sediments. Porosity in Unit I decreases rapidly from 80% at the surface to 45 % at ~130 mbsf, consistent with a high rate of compaction ($\Phi \approx 75 * \exp(-z/250)$). In Units II & III (below 130 mbsf), porosity continues to decrease to ~35% at ~995 mbsf consistent with compaction at a slower rate ($\Phi \approx 50 * \exp(-z/3000)$).

Carbonate abundance is generally below 15 wt% but in Unit I (0 - 74 mbsf) where mean value is ≈ 40 wt%. XRD clay mineralogy by Yu et al. (2019) shows that at top of Unit I ($z < 43$ mbsf), smectite (≈ 60 %) is the primary clay component with Illite (≈ 30 %) similar to U1456.

171 The deeper sediments have not been specifically studied for clay mineralogy. However given
172 the tectono-geographic and lithological proximity with U1456, it is very likely that the
173 abundances of the different types of clays in U1457 are very close to those of Site 1456. Thus,
174 smectite would be more abundant than illite in Unit 1 and at the top of Unit 3, whereas illite
175 would be more abundant than smectite in Unit 2 and at the base of Unit 3.
176
177 **III) Chemical chracteristics of the pore fluids from Sites U1456 and U1457**
178 During Leg 355, immediately after recovery, pore fluids were extracted from the sediment
179 by squeezing core sections (Manheim, 1966), filtered through 0.45 μm and then stored in
180 plastic vials. The squeezing on board the ship was conducted at very low pressure (< 200 MPa)
181 which ensured that no or very little chemical and isotope fractionations occurred in the
182 extracted pore fluids (Coleman et al., 2001; Mazurek et al., 2015; Bonifacie et al., 2007). The
183 shipboard pore fluid extractions and analyses of Chloride, Sodium, Calcium, Magnesium,
184 Potassium, Alkalinity, pH, Sulfate and Bromide concentrations were carried out on board
185 following the protocols of Gieskes et al. (1991), Murray et al. (2000), Pandey et al. (2016d) and
186 the IODP user manuals for shipboard instrumentation. Chemical data are taken from Pandey et
187 al. (2016b, & c). $^{87}Sr/^{86}Sr$ ratios are taken from Carter et al. (2017). All these data from
188 published literature are shown in Figure 1.
189 *III.1 Concentration in chloride, [Na^+], [Na^+]/[Cl^-] and [Br^-]/[Cl^-] molar concentration ratios:*
190 Chlorinity and Na^+ profiles are similar at both wells. They are generally within 2 %, close to
191 seawater concentrations, ~ 558 mM and ~ 480 mM respectively. They do not vary much with
192 depth. Towards the bottom of the two sedimentary piles, in Unit III, the profiles are more noisy.
193 Similarly, the [Na+]/[Cl-] ratios are consistent in both sites and remain very close to that of
194 seawater. The [Br^-]/[Cl^-] ratios increase rapidly below the water-sediment interface in Unit I,
195 then more slowly in Unit II, becoming constant at depth in Unit III. Most of the increase in the

196 [Br-]/[Cl-] ratio is due to the variation in bromide, the variation in chloride being very small.
197 The Br/Cl ratios are consistent with the organic carbon concentrations in these sites. They are
198 high in unit 1 and markedly lower below, in units 2 and 3. Bromide enrichment of this kind is
199 often found in sediments, It may be caused by the release of Br^- from the solid part of organic-
200 rich sediments to the pore fluids during diagenesis (Kendrick, 2018). A further contribution to
201 this Br enrichment could be the filtration of the fluid through the clays. This would lead to an
202 accumulation of Br- upstream of the clay membrane relative to Cl- if the clay membranes allow
203 less Br- than Cl- to pass through.

204 *III.2 Cations:* [Ca^{2+}] and [Mg^{2+}] depth profiles are similar at U1456 and U1457. From the top
205 to the bottom of the sedimentary piles, the main changes are: In Unit I, rapid decrease of Ca^{2+}
206 and Mg^{2+}. In Unit II, increase of Ca^{2+} at top then decrease of Ca^{2+} at the bottom; stability of Mg^{2+}.
207 In Unit III & IV, increase in Ca^{2+}, slight decrease in Mg^{2+}.

208 *III.3 Strontium:* $^{87}Sr/^{86}Sr$ of Carter et al. (2017) show organised changes with
209 lithostratigraphy. In summary, from top to bottom, in Unit I, $^{87}Sr/^{86}Sr$ is at the seawater value
210 (0.7092). Downwards, in Unit II mainly, $^{87}Sr/^{86}Sr$ is increased, with a maximum at ~ 200 mbsf
211 in unit II. At the bottom, $^{87}Sr/^{86}Sr$ is strongly decreased. At U1456, at the base of Unit III and in
212 Unit IV, $^{87}Sr/^{86}Sr$ is constant at ≈ 0.7085. These changes show that Strontium in the pore fluids
213 is clearly influenced by water-minerals interactions that resulted in radiogenic Sr inputs from
214 radiogenic detrital minerals in the upper part (Units I & II) and contributions of Sr less
215 radiogenic than that of seawater (from Paleogene carbonates) in the lower part (Units III & IV).
216 Indeed, the deep $^{87}Sr/^{86}Sr$ ratios are slightly lower than the contemporaneous value.
217

218 **IV) Cl isotope methods**

219 *IV.1 Fluid sampling:* We selected 25 pore fluids from Site U1456 and 20 pore fluids from Site
220 U1457, which were sampled at regular depth intervals (every 50 meters) from 2 mbsf below
221 the seawater-sediment interface to the bottom of the sedimentary piles (≈ 800 mbsf).
222 *IV.2 Chlorine isotope measurements:* All the pore fluids were analysed for their $\delta^{37}Cl$ at the
223 Institut de Physique du Globe de Paris (IPGP). We used the AgCl-CH_3Cl method (Kaufmann et al.,
224 1984; Eggenkamp, 1994) with improvements made at IPGP (Godon et al., 2004b). Gaseous
225 CH_3Cl was measured for $\delta^{37}Cl$ using a dual-inlet gas source mass spectrometer (Delta plus XP or
226 Delta V from ThermoFisher). The results are reported using the $\delta^{37}Cl$ versus SMOC (Standard
227 Mean Ocean Chloride). Over the course of the study, the external reproducibility of the
228 Atlantique 2 seawater chloride reference was ± 0.025 ‰ (1σ, n = 48). This is comparable, if not
229 better than, to the routine long-term precision reach at IPGP over the past two decades (e.g.,
230 Godon et al., 2004a, Bonifacie et al, 2005, Bonifacie et al.2007, Li et al., 2015; Eggenkamp et al.,
231 2016; Giunta et al. 2017, Agrinier et al., 2019 and 2021) .
232
233 **V) Results**
234 Isotope compositions of the pore fluids are given in the Table 1. Figure 2 shows the depth
235 profiles of the pore fluid chloride chlorine isotopic compositions ($\delta^{37}Cl$). In the $\delta^{37}Cl$ depth
236 profiles, decreasing trends are observed between the seawater boundary value at $\delta^{37}Cl$ = 0 at
237 the top of the sedimentary piles and the minima systematically located at the deepest depths
238 and in lithologies with abundant clays ($\delta^{37}Cl$ = -2.50 ‰ at 741.45 mbsf in U1456 and -1.40 ‰
239 at 794.4 mbsf in U1457, Figure 2). At both sites, the shapes of the trends are similar and
240 correlate with the lithostratigraphy. Transitions between lithostratigraphic units are marked
241 by a break in the slope of the trends. The smoothness of the trends decreases with depth (the
242 deepest parts of the trends are more noisy). Within units, the slope of the trend is constant. In
243 Unit 1, U1456 and U1457 trends have similarly steep slopes (-0.7 ‰ per 100 m in U1456 and -

0.5 ‰ per 100 m in U1457). Below, in Unit II, the slopes are clearly reduced to very small values (-0.2 ‰ per 100 m in U1456 and -0.02 ‰ per 100 m in U1457). At the bottom, in Unit III, the slope values are increased (-0.3 ‰ per 100 m in U1456 and -0.2 ‰ per 100 m in U1457). The difference between the two profiles is due to unit II. In U1456, $\delta^{37}Cl$ continues to decrease, whereas it remains constant in U1457.

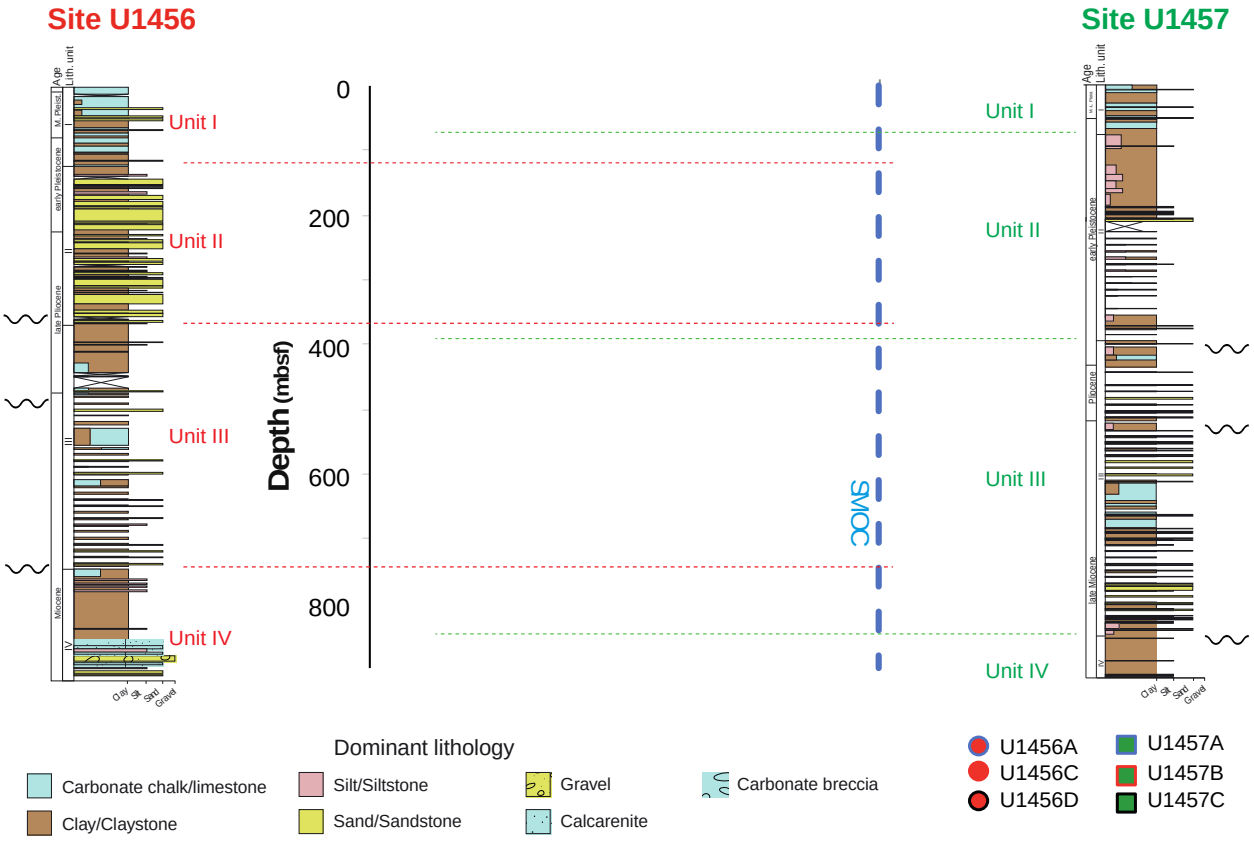

Figure 2: *Profiles of the chlorine stable isotope ratio of chlorides ($\delta^{37}Cl$) of the pore fluids sampled in Sites U1456 and U1457 (data from Table 1). Lithostratigraphic logs (U1456 left and U1457 right) are from Pandey et al. (2016b and c). Horizontal dashed lines, (red for U1456 and green for U1457) delimit the lithostratigraphic units (I, II, III & IV). SMOC is the mean seawater chlorine isotope compostion.*

Overall, the changes in the isotopes and chemical compositions of pore fluids of U1456 and U1457 fits in with changes identified since early works on sediment pore fluids (Lawrence et al.,

1975; Gieskes and Lawrence, 1976). They are increases in Ca^{2+}, decreases in Mg^{2+}. The magnitudes of these changes are modest. Mg^{2+} is only reduced by only 30 mM, $\delta^{37}Cl$ by -1.5 ‰, Ca^{2+} is increased by 5 mM compared to pore fluids of other kilometre thick sedimentary pile, where these parameters are much more changed. The largest gradients of changes are systematically located in Unit I, i.e., in the upper 100 metres just below the sediment-seawater interface. Similarly, the Br/Cl ratios of interstitial fluids also show this pattern of variation gradient damping as depth increases.

In general, at Sites U1456 and U1457, there is good agreement between the geochemical characteristics of the pore fluids and the lithology. Good agreement is also observed between the porosity and the chloride $\delta^{37}Cl$ (Figure 3). Breaks in the profiles of porosity and of $\delta^{37}Cl$ of chlorides occur at the same depths, systematically at the transitions between lithological units.

In terms of chloride geochemistry, the pore fluids exhibit the usual chloride geochemical features recorded in the vast majority of oceanic clay-rich sedimentary sites (Agrinier et al., 2019 and 2021). They are:

i) chloride profiles with $\delta^{37}Cl$ steadily decreasing from the seawater value ($\delta^{37}Cl$ = 0 ‰) while chloride concentrations remain quite close to that of seawater (≈ 558 mM). The slope of the $\delta^{37}Cl$ profiles is steep just below the seawater-sediment interface and gradually decreases with depth.

ii) loss of smoothness of the $\delta^{37}Cl$ profiles as a function of depth. The increase in $\delta^{37}Cl$ noise in the deeper parts could be the result of late disturbing processes of relatively small magnitude that develop as the sediment ages.

These two points suggest that the process of lowering the $\delta^{37}Cl$ is mainly in the sediments, below the interface between seawater and the sediment. Another possibility could be that the process develops quite deep and involves large chlorine isotope fractionations. The steep upper parts of the $\delta^{37}Cl$ profiles would then result from mixing with seawater favoured by a relatively

high permeability below the water-sediment interface. Furthermore, the process of lowering $\delta^{37}Cl$ has little or no impact on the chloride concentration of pore fluids.

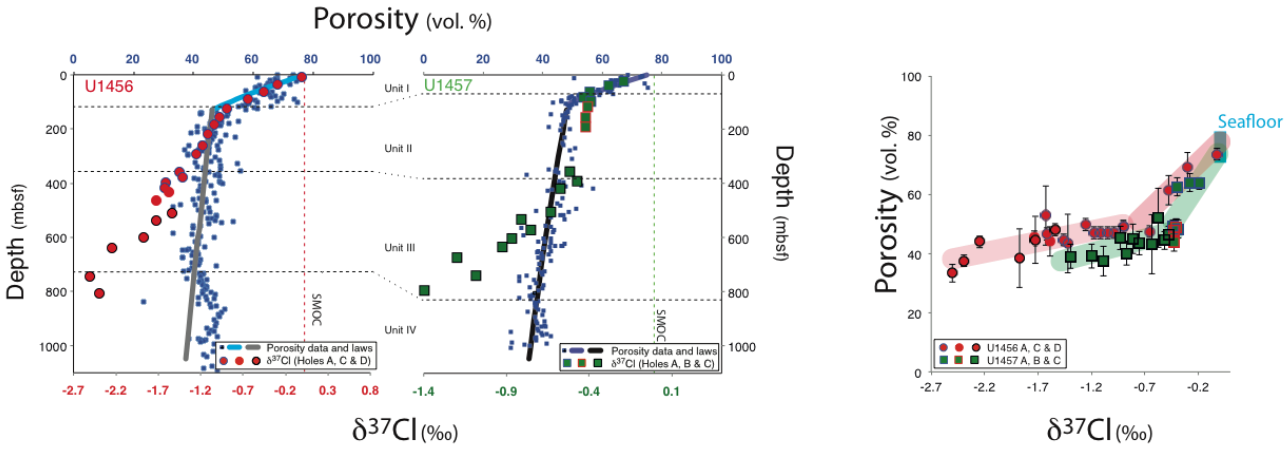

Figure 3: *U1456 and U1457 porosity and $\delta^{37}Cl$ depth profiles (**Left and center**). Porosity data are from Pandey et al. (2016b & c). The inset for Site U1456 shows the upper part of the porosity and $\delta^{37}Cl$ depth profiles. U1456 porosity data, Φ, are fitted with compaction law $\Phi \approx 75 * exp(-z/400))$ in Unit I ($z \leq 120$ mbsf) and with compaction law $\Phi \approx 48 * exp(-z/5500)$ in Units II, III & IV ($z > 120$ mbsf). U1457 porosity data, Φ, are well fitted with compaction law $\Phi \approx 75 * exp(-z/250))$ in Unit I ($z < 100$ mbsf) and with compaction law $\Phi \approx 50 * exp(-z/3000)$ in Units II & III ($z > 100$ mbsf.*

VI) Discussion

Because chlorides are highly soluble and because they are the second most abundant compound in oceanic sedimentary pore fluids, after water, the decrease in $\delta^{37}Cl$ of pore fluid chlorides places important constraints on the history of these fluids. Whatever the process causing the decrease, the conservation of stable isotopes of chlorine requires that it is due to either the preferential removal of ^{37}Cl isotopes from the chlorides of the original pore fluid (seawater) or by the addition of ^{37}Cl-depleted chlorides. This latter possibility has been considered in previous works (Ransom et al., 1995; Spivack et al., 2002; Wei et al., 2008) for the sediments of subduction zone accretionary prisms: fluids of deep origin, depleted in ^{37}Cl, produced in the subduction zone, entered the sedimentary pile from greater depths. However, this is very difficult to consider in the present study because advection must have occurred

306 under unfavourable hydrogeological conditions with porosity and permeability decreasing with
307 depth. Considering the shape of the $\delta^{37}Cl$ and [Cl^-] profiles, the potentially advected fluid would
308 have chlorides with $\delta^{37}Cl$ lower than the lowest measured $\delta^{37}Cl$ value (-2.50 & -1.40 ‰ in Sites
309 U1456 & U1457, respectively) and higher chlorinity than the highest measured value (573 and
310 568 mM, respectively). Futhermore, this advection of fluid up through the sedimentary pile
311 does not operate for the many other sedimentary piles, not associated with subduction zones,
312 that nevertheless systematically show the depletion in of their pore fluid chlorides (Agrinier et
313 al., 2021). The ubiquity of the ^{37}Cl depletion of chloride in sediments confirms that the process
314 fractionating the chlorine isotope of chlorides is local and specific to the type of the sediments.
315 This results in the loss of ^{37}Cl-enriched chlorides from the pore fluids.
316 Further constraints can be provided by studying the budget of chlorides in sediments. First,
317 we describe the methodology used to establish the chlorine budget in sediments. We illustrate
318 this using data from Sites 1456 and 1457 of Leg 355. We then provide additional constraints
319 from a review of the geochemical processes that fractionate chlorine isotopes and an open
320 system ^{37}Cl-enriched chloride loss from the pore fluids. Finally, we calculate the amount of
321 missing ^{37}Cl-enriched chlorides required to compensate for the ^{37}Cl-depletion of pore fluid
322 chlorides, assuming that sediment pore fluids were originally seawater trapped on the seafloor.
323 This methodology is used to determine the chloride budget at 22 other IODP drilled sites in
324 oceanic sediments of different tectonic settings (Table 2).
325
326 **VI.1 Budget of chloride in the sediments**
327
328 *The pore fluids:* In this section we calculate the amount of pore fluids present in the sediment
329 and the amount of chlorides contained in the pore fluids. For a vertical sediment column of 1
330 square meter horizontal surface (S = 1 m^2), the volume of pore fluids, $V_{porefluid}$, is given by

$$V_{porefluid} = \int_0^{depth\ max} \Phi_z \,.S.\,dz \qquad (1)$$

where Φ_z is the porosity law (from Figure 3) and dz is the depth element (m). $V_{porefluid}$ are 457 and 454 m^3 for a vertical sediment column of ≈ 1 km in height in Sites U1456 and U1457 respectively (Table 2). Then, $Q_{porefluid}$, the amount of pore fluid (expressed as water) can then be calculated as follows:

$$Q_{porefluid} = V_{porefluid}\, C_{H_2O} \qquad (2)$$

where C_{H2O} is the concentration of water in the pore fluid (≈ 54.9 kmoles of H_2O/m^3 using concentration of water in seawater at 0.965 kg H_2O per Kg of seawater and density at 1023.6 Kg/m^3). $Q_{porefluid}$ values are 25081 and 24891 kmoles of water for the U1456 and U1457 sediment columns respectively (Table 2).

The amount of chloride in pore fluids, $Q_{Cl\ porefluid}$, is given by :

$$Q_{Cl\ porefluid} = \int_0^{depth\ max} \Phi_z \,.S.\,[Cl^-]_z \,.dz \qquad (3)$$

where $[Cl^-]_z$ is the chloride concentration in the pore fluid at depth z (in kmoles of chloride/m^3). Then $Q_{Cl\ porefluid}$ are 252 and 246 kmoles of chlorides for the U1456 and U1457 sediment columns respectively (Table 2). The mean $\delta^{37}Cl$ values of the pore fluid chlorides are given by:

$$\delta^{37}Cl_{porefluid} = \frac{1}{Q_{Cl\ porefluid}} \int_0^{depth\ max} \Phi_z \,.S.\,[Cl^-]_z \,.\delta^{37}Cl_z.dz \qquad (4)$$

where $\delta^{37}Cl_z$ is the isotopic composition of the chloride profile versus depth (in ‰ vs. SMOC). The mean $\delta^{37}Cl$ values of chlorides of the sediment columns U1456 and U1457 are -1.59 and -0.73 ‰, respectively (Table 2). The mean [Cl^-] values, *in mole* Cl per Kg of porefluid, are given by :

$$[Cl^-]_{porefluid} = \frac{Q_{Cl\ porefluid}}{Q_{porefluid}\ \rho_{seawater}} \qquad (5)$$

with $\rho_{seawater}$ = 1023.6 kg.m^{-3}

The solid fraction: The solid fraction of the U1456 and U1457 sediments consists of components that contain very small amounts of chlorine in their structure. As reported in Pandey et al. (2016a, b & c), they are mainly carbonates, clays (chlorite and illite ≥ smectite), detrital minerals (quartz, feldpars, micas, and rare hornblende, glaucophane, kyanite, tourmaline, clinopyroxene, apatite, and glauconite). Total organic carbon varies between 0 and 2.6 wt% (mean value ≈ 0.5 wt%). In these constituents, chlorine content is generally lower than 200 ppm Cl (Ransom et al., 1995; Wei et al., 2005 and 2008, Bonifacie et al., 2008; Barnes et al., 2009; Kendrick, 2018) but can be up to the few percent level in rare high-temperature detrital minerals such as apatite, micas, and amphiboles. Serpentine minerals, absent in these sediments, may store up to 5000 ppm Cl.

In the sediment column, the amount of chloride in the solid part of the sediment is given by:

$$Q_{\mathrm{Cl\ solid}} = \frac{V_{\mathrm{solid}} \cdot \rho_{solid} \cdot C_{\mathrm{Cl\ solid}}}{0.0355} \qquad (6)$$

with $V_{solid} = Depth\ max\ .\ S - V_{porefluid}$ (7)

where $C_{Cl\ solid}$ is the concentration of Cl in the solid (≤ 2 10^{-4} kg of Cl/kg of solid = 200 ppm), V_{solid} is the volume of solid in the sediment (V_{solid} = 543 and 546 m^3 for the 1 km high sediment column of Sites U1456 and U1457 respectively) and ρ_{solid} is the density of the solid part of the sediment (≈ 2800 ± 100 kg/m^3 of solid). Then we get $Q_{Cl\ solid}$ maxima values at 8.6 and 8.6 kmoles of Cl in Sites U1456 and U1457, respectively (Table 2). The isotopic composition of chlorine in the solid fraction of sediments has rarely been measured. Generally, it is depleted in ^{37}Cl compared to seawater. Barnes et al. (2008) measured $\delta^{37}Cl$ of "structurally bound chlorides" at $\delta^{37}Cl$ = -1.1 ± 0.7 ‰ (15 sediment samples of Leg 125, 129 & 189).

Chloride budget in the sediment:

In these sediments under consideration, chlorine is mainly present as chlorides in the pore fluids. Chlorine in the solid fraction is only at the level of a few percent (≤ 3 %), which is two orders of magnitude less than the amount of chloride in the pore fluids. As shown above the pore fluids in sediments lose ^{37}Cl-enriched chlorides and the amount of that loss can be assessed by looking at the chlorine isotope budget of chlorides in the pore fluids. This budget approach depends only on the chloride and isotope conservation equations which are uncontroversial. The nature of the geochemical process fractionating the chlorine isotopes, which may be controversial, does not come into play at this stage and will be discussed later.

Missing chlorides: The loss of ^{37}Cl-enriched chlorides from the pore fluids can be evaluated in terms of the quantity of chlorides ($Q_{Cl\ loss}$) and the chlorine isotope ratios ($\delta^{37}Cl_{loss}$) by examining the chloride budget including chlorine isotopes. By comparing the initial amount of of chlorides ($Q_{\sum Cl}$) with the amount of chlorides in the fluid ($Q_{Cl\ porefluid}$), a conservation equation for chlorides can be written:

401

402 $$Q_{\sum Cl} = Q_{Cl\ porefluid} + Q_{Cl\ loss} \qquad (8)$$

403

404 and a conservation equation for the chlorine isotopes of the chlorides can be written:

405

406 $$Q_{\sum Cl}\,\delta^{37}Cl_{\sum Cl} = Q_{Cl\ porefluid}\,\delta^{37}Cl_{porefluid} + Q_{Cl\ loss}\,\delta^{37}Cl_{Cl\ loss} \qquad (9)$$

407

408 where $Q_{Cl\ loss}$ and $\delta^{37}Cl_{loss}$ is the pair of unknowns that cannot be evaluated independently
409 because we have only one independent equation, the unknowns ($Q_{Cl\ loss}$ and $\delta^{37}Cl_{loss}$) are
410 coupled. The unknown $Q_{\sum Cl}$ is eliminated via equation 8. All the other parameters ($\delta^{37}Cl_{\sum Cl}$,
411 $\delta^{37}Cl_{porefluid}$) have known values (assuming that the original pore fluids were seawater, $\delta^{37}Cl_{\sum Cl}$
412 = $\delta^{37}Cl_{seawater}$). Then, P, the proportion of chloride lost is given by :

413

414 $$P = \frac{Q_{Cl\ loss}}{Q_{\sum Cl}} = \frac{(\delta^{37}Cl_{\sum Clseawater} - \delta^{37}Cl_{porefluid})}{(\delta^{37}Cl_{loss} - \delta^{37}Cl_{porefluid})} \qquad (10)$$

415

416 which has an hyperbolic dependence on $\delta^{37}Cl_{loss}$ (P = A/$\delta^{37}Cl_{loss}$, Figure 4). This shape reveals
417 an antagonistic relationship between the amount of chloride lost, P, and the $\delta^{37}Cl_{loss}$: a large
418 chloride loss (> 50 %) is associated with small $\delta^{37}Cl_{Cl\ loss}$ (< 1.5 ‰), that is small chlorine
419 isotope fractionation between lost chlorides and porefluid chlorides whereas small loss (<
420 10 %) is associated with large $\delta^{37}Cl_{Cl\ loss}$ (> 8 ‰), i.e. large chlorine isotope fractionation
421 between lost and porefluid chlorides.
422 This relationship between chlorine isotope fractionation and the amount of chloride lost
423 significantly reduces the range of possible processes that can be invoked to explain the
424 decrease in chloride $\delta^{37}Cl$.

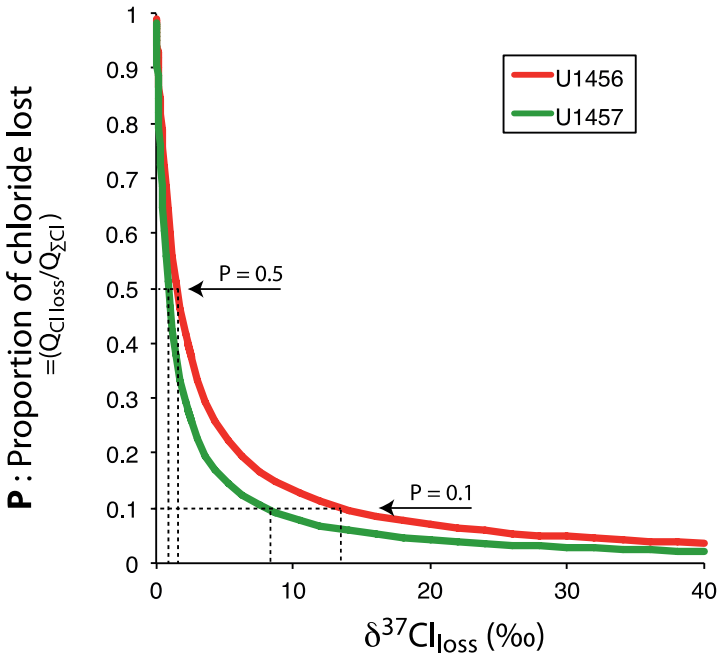

Figure 4 *: Relationship between P, the proportion of chloride lost from the porefluid and* $\delta^{37}Cl_{loss}$*, the mean* $\delta^{37}Cl$ *value of the lost chlorides. The model is based on the evolution of the* $\delta^{37}Cl$ *of chlorides in pore fluids from the initial* $\delta^{37}Cl$ *at seawater* $\delta^{37}Cl$ *(= 0 ‰) to a mean value of* $\delta^{37}Cl_{porefluid}$ *values of -1.51 ‰ (U1456) and -0.88 ‰ (U1457). Small P's are associated with large* $\delta^{37}Cl_{loss}$ *and conversely large P's with small* $\delta^{37}Cl_{loss}$*. A 50 % loss of chloride (P = 0.5, upper horizontal dashed line) requires a loss of* ^{37}Cl*-enriched chlorides with mean values of* $\delta^{37}Cl_{loss}$ *values of 1.5 ‰ and 0.9 ‰ for Sites U1456 and U1457, respectively. A 10 % loss (P = 0.1, lower horizontal dashed line) requires a loss of* ^{37}Cl*-enriched chlorides with mean values of* $\delta^{37}Cl_{loss}$ *values of +13.6 ‰ and +7.9 ‰ respectively.*

<u>*Chlorine isotope fractionation between pore fluid chlorides and lost chlorides*</u>

Additional constraints may be provided by a review of chlorine isotope fractionations between chlorides and phases that could incorporate lost chlorides. The thermodynamic properties of isotopes dictate that chlorine isotope fractionation factors, are close to 1.000 to a few permil, at temperatures above 0°C regardless the process (Urey, 1947; Richet et al., 1977; Schauble et al., 2003; Balan et al., 2019; Liu et al., 2021). Indeed, such ranges of chlorine isotope fractionation are observed in natural and experimental systems (Desaulnier et al; 1986; Lavastre et al., 2005; Eggenkamp and Coleman, 2009; Sharp et al., 2010; Richard et al., 2011; Giunta et al., 2017a,b). For the ion filtration process of chlorides in clay-rich oceanic sediments

undergoing compaction, α values in the range of 1.00025 to 1.008 are proposed (Agrinier et al., 2021). Larger chlorine isotope fractionations are produced when chlorine is oxidised to an oxydation number of +2 to +7. Values of up to 1.07 have been obtained for the fractionation between chloride and perchlorate (Urey, 1947; Schauble et al., 2003; Ader et al., 2008) but these require extremely oxidizing conditions in contrast to those of oceanic sediments, which are reducing.

By writing an open system chlorine loss model, a Rayleigh distillation law, the chlorine isotope fractionation can be related to the proportion of chlorine lost (P). It gives the $\delta^{37}Cl$ of the pore fluids as the loss of ^{37}Cl-enriched chlorides increases :

$$\delta^{37}Cl_{porefluid} = \delta^{37}Cl_{seawater} + \Delta^{^{37}Cl/^{35}Cl}_{loss-porefluid} Log_e(1-P) \qquad (11)$$

with $$\Delta^{^{37}Cl/^{35}Cl}_{loss-porefluid} = 1000 Log_e\left[\alpha^{^{37}Cl/^{35}Cl}_{loss-porefluid}\right]$$

This modelling shows that for small $\alpha^{37Cl/35Cl}_{loss\text{-}porefluid} \leq 1.008$, a large portion of the chlorides must be lost from the sediment pore fluids (Figure 5). At least 35%, P= 0.35, for $\alpha^{37Cl/35Cl}_{loss\text{-}porefluid} = 1.008$ is required to produce ^{37}Cl depletions up to $\delta^{37}Cl$ = -2.51 ‰. The smaller the $\alpha^{37Cl/35Cl}_{loss\text{-}porefluid}$, the larger the loss. Obviously, the model predicts that the loss is enriched in ^{37}Cl. The smaller the $\alpha^{37Cl/35Cl}_{loss\text{-}porefluid}$, the lower the ^{37}Cl enrichment of the loss. If the $\alpha^{37Cl/35Cl}_{loss\text{-}porefluid}$ is very large, greater than 1.02, chloride loss is low (P ≤ 0.2), but this requires oxidizing conditions, to produce ClO_n, that are not compatible with the reducing conditions found in ocean sediments.

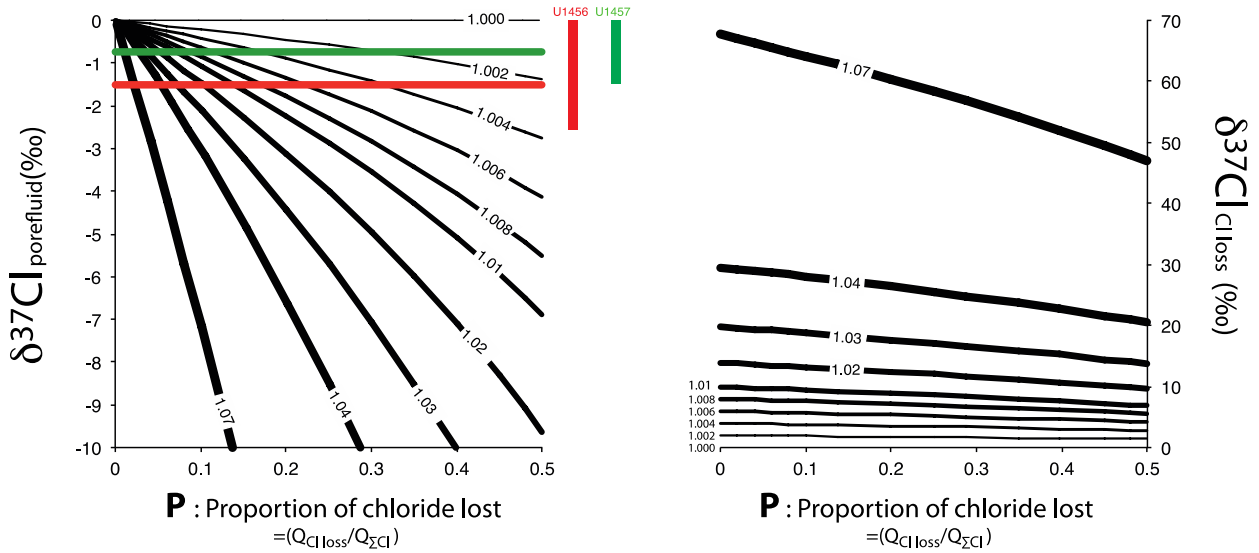

Figure 5*: Open system model of chlorine loss from the pore fluids (equation 11). It calculates the $\delta^{37}Cl$ of the chloride remaining in pore fluids in the sediment (left) and the $\delta^{37}Cl$ of the lost chlorides (right) as a function of the proportion of chloride lost from the porefluid (P). The curves are obtained for a range of $\alpha_{loss\text{-}porefluid}$ ranging from 1.000 to 1.07. This range covers the known fractionation factor values for chlorine isotopes for a lot many processes including (diffusion, ion filtration, gravitational settling, for small values (≤ 1.01) and larger values, up to 1.07 when chloride get oxidised to a redox state of +7). The ranges of $\delta^{37}Cl_{pore\ fluids}$ in U1456 and U1457 sediments are shown as vertical red and green bars respectively on the right. The red and the green horizontal lines are the mean $\delta^{37}Cl_{pore\ fluids}$ values of chlorides for Sites U1456 and U1457, respectively. The U1456 and U1457 $\delta^{37}Cl_{pore\ fluids}$ data can be explained by small $\alpha_{loss\text{-}porefluid} \leq 1.002$ and large proportions of chloride lost from the porefluid (P).*

If $\alpha^{37Cl/35Cl}_{loss\text{-}porefluid}$ is very large, greater than 1.02, the chloride loss is small (P ≤ 0.2), but the thermodynamic conditions it requires (oxydation to produce ClO_n) are not compatible with those found in oceanic sediments (reducing).

Using the Cl filtration isotope mass balance model (Closed sedimentary pile : CSP), described in appendix B of Agrinier et al. (2019), the Sites U1456 and U1457 pore fluids can be fitted with small $\alpha^{37}Cl/^{35}Cl_{lost\text{-}porefluid}$ ranging between 1.00025 and 1.0025 (Figure 6). Note that at the top of the sediment column, this model has a boundary condition to set chlorinity and $\delta^{37}Cl$ to seawater values. This condition is imposed to represent the rapid exchange of chlorides across

the sediment-seawater interface (Agrinier et al., 2019). It erases the accumulation of ^{37}Cl-enriched chlorides, which are expelled from the bottom of the column where ^{37}Cl-depleted chlorides remain. The small $\alpha^{37}Cl/^{35}Cl_{lost\text{-}porefluid}$ values were expected because i) the ^{37}Cl-depletion of chlorides are small, less than -2.5 ‰ from the seawater' $\delta^{37}Cl$ value and ii) the nature of sediments with low clay content. Furthermore, the model shows that for such small α values,

$$P = F_{Chloride} = 1 - \left[\frac{\phi_z}{\Phi_0}\frac{(1-\Phi_0)}{(1-\phi_z)}\frac{[Cl^-]_z}{[Cl^-]_{seawater}}\right] \qquad (12)$$

to produce the most ^{37}Cl-depleted pore fluids ($\delta^{37}Cl \leq -0.5$), the proportion of initial chloride loss, P, equal to $F_{chloride}$ of Agrinier et al. (2019; 2021), must be greater than 0.4.

Then large proportions of the initial chloride, ≥ 40 %, would have been lost from the pore fluids and hence from the sediments. This is consistent with the open system modelling reasoning developed above, which shows that large fractions of the original chlorides must have been lost (Equation 11, Figure 6).

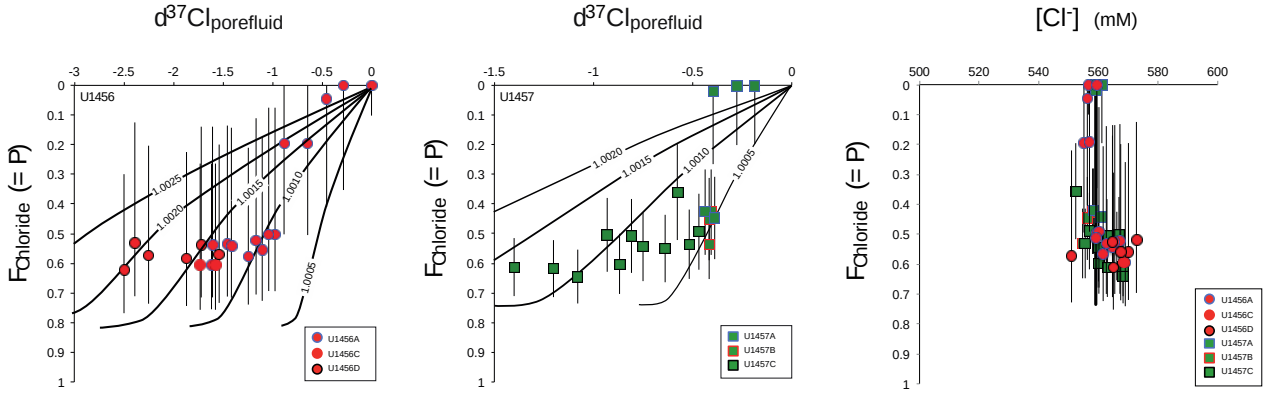

Figure 6: *The $\delta^{37}Cl_{Cl\ porefluid}$ – $F_{chloride}$ and [□]□ – $F_{chloride}$ relationships for pore fluids from Sites U1456 and U1457. The data can be fitted with the Cl filtration isotope mass balance model curves (closed sedimentary pile : CSP of Agrinier et al., 2019) with small value of chlorine isotope fractionation between the lost chloride and the pore fluid chloride ($\alpha^{37}Cl/^{35}Cl_{lost\text{-}porefluid}$) ranging between 1.0025 and 1.00025 shown as black labelled curves (left and centre). This 1D model uses*

the boundary condition where the column is open at the top to allow complete chloride exchange between sediment and seawater (CSP model of Agrinier et al., 2019). Error bars on $F_{chloride}$ values are due to the uncertainty on the Φ_0 values of the compaction laws. In the [□l□ – $F_{chloride}$ plot (right), all the model curves with this range of α are plotted on the same vertical black line at 558 mM.

Losses of fluids and chlorides from the sediment :

$V_{\text{lost porefluid}}$ can be estimated from a fluid balance. It is obtained by substracting the amount of porefluid of the current compacted sediment column, $V_{\text{porefluid}}$, from the amounts of porefluid in the decompacted sediment column, $V_{\text{porefluid decompacted}}$. The decompacted sediment column thickness, $H_{\text{decompacted}}$, can be estimated assuming that the volume of solid, V_{solid}, is unchanged during compaction of the sediment, according to :

$$H_{decompacted} = \frac{H_{present\ day}}{(1-\phi_0)} \qquad (13)$$

(Perrier and Quiblier; 1974; Lucazeau and Le Douaran, 1985). This relationship assumes that the compaction law, $\Phi_{□}$, has remained the same since sediments started to accumulate. It allows to get an estimate of the amount of the volume of the fluid in the decompacted sediment column, $V_{\text{porefluid decompacted}}$, according to :

$$V_{porefluid,decompacted} = \Phi_0 . S . H_{decompacted} \qquad (14)$$

where S = 1m². Then the volume of lost porefluid, $V_{\text{lost porefluid}}$, that has been expelled from the sediment since the sediment started to accumulate is given by the porefluid budget :

$$V_{lost\ porefluid} = V_{\text{porefluid decompacted}} - V_{\text{porefluid}} \qquad (15)$$

In the same way the amount of lost chloride from the sediment, $Q_{\text{Cl lost}}$ can be estimated from the chloride balance :

$$Q_{Cl\ lost} = Q_{Cl\ decompacted\ sediment} - Q_{Cl\ pore\ fluid} \quad (16)$$

where the amount of chloride in the porefluid for the decompacted sediment column is given by :

$$Q_{Cl\ decompacted\ sediment} = \Phi_0 . S. [Cl^-]_{seawater} . H_{decompacted} \quad (17)$$

$Q_{Cl\ loss}$ values are of about 187 ± 45 and 231 ± 50 kmoles of chlorides. Then $\delta^{37}Cl_{Cl\ loss}$ are 2.3 ± 0.15 ‰ and 0.8 ± 0.15 ‰ respectively because the lost chlorides must be ^{37}Cl-enriched in order to compensate for the ^{37}Cl-depletion of the chlorides of the pore fluids (mean δ^{37}Cl of -1.59 and -0.73 ‰, respectively, Table 2). These chloride losses are very large, about 40 % of the "original" chlorides. They are the same magnitude as the $Q_{Cl\ porefluid}$, the amount chlorides still present in the pore fluids (≈ 250 kmoles for the U1456 and U1457). The mean chlorinity of the lost pore fluids can be calculated with

$$[Cl^-]_{lost\ pore\ fluid} = \frac{Q_{Cl\ lost}}{V_{lost\ porefluid} * \rho} \quad (18)$$

where ρ is the density of pore fluid (≈ 1026 Kg.m^{-3}). They are, respectively, 0.512 and 0.562 Mole of chloride per kg for U1456 and U1457, and very close to that of seawater (≈ 0.558 Mole of chloride per kg). This consistency of chlorinities is expected in light of the chlorinities of the pore fluids, which have remained very close to that of seawater (Figure 1). Then the process that fractionates the chlorine isotopes of chlorides in the porefluids of the sediments would not have a large impact on the chlorinity.

A sink can be proposed. As mentioned above, the current knowledge of the geochemistry of chlorides indicates that there is no reservoir in the sediment capable of sequestering that much of lost chlorides. The lack of storage capacity for chlorides in the sediment then leads to the conclusion that they have been expelled into the overlying seawater. This expulsion of

555 chlorides from the sediment is necessary to produce the decrease of the $\delta^{37}Cl$ of pore fluid
556 chlorides with depth. Chlorine isotope fractionation at the sediment-water interface, which
557 would force ^{37}Cl-enriched chlorides into the seawater as the sediment settles, does not have the
558 capacity to produce the observed progressive decrease in $\delta^{37}Cl$ with depth. Then the chlorine
559 isotope fractionation then takes place in the sediment.

560 An estimate of this mean flux of ^{37}Cl-enriched chlorides out of the sediment pile is given by

561 $$Flux_{expelled\ chloride} = \frac{Q_{Cl\ loss}}{age\ oldest\ sediment} \quad \text{(in Mole of chloride. m}^{-2}\text{. Kyr}^{-1}\text{)} \quad (19)$$

562 The flux of chloride expelled out of the sediment 17.0 and 23.1 (± 5) moles of chloride per
563 square metre per 1000 years for Sites U1456 and U1457 (using $Q_{Cl\ lost}$ values, about 187 and
564 231 kmoles of chlorides, Table 2). Since this lost chloride flux cannot be pure chloride, there
565 must be a vector transporting ^{37}Cl-enriched chloride out of the sediment. The only chloride
566 carrier available in the sediment is the pore fluid water. Therefore, the expulsion of pore fluid
567 from the sediment to the seawater is a necessary consequence to produce the decrease in $\delta^{37}Cl$
568 of chlorides in the sediment.

569 The lost fluid flux would be 1783 and 2201 moles of water per 1000 years per square metre
570 for Sites U1456 and U1457 respectively, using :

$$Flux_{expelled\ fluid} = \frac{V_{porefluid}\ C_{H_2O}}{age\ oldest\ sediment} \quad (20)$$

571 where C_{H2O} is the concentration of water in the pore fluid (54.9 kmoles of H_2O/m^3). This is in
572 contrast to models of compaction of sediments which suggest that, at the seawater-sediment
573 interface, the fluid enters the sediment, although not as fast as the solid (Berner, 1980;
574 Hutchinson, 1985; Boudreau, 1997) but such conditions cannot explain the decrease in $\delta^{37}Cl$ of
575 chlorides below the seawater-sediment interface. Another implication of this outflow of

chlorides into the seawater is that imposed by the condition of electroneutrality of the ion flux. The outflow of negative charges from chlorides must be accompanied by an outflow of positive charges carried by cations (Na^+, Ca^{2+}, Mg^{2+}, ...) or by an inflow of negative charges which may be electrons and anions. As the Na^+/Cl^- ratio of the pore fluids remains very close to that seawater (Figure 1), chloride losses are most likely coupled to sodium ion losses.

V.2 Chloride exchanges between sediments and seawater

In Table 2, we calculated the budgets of pore fluids and pore fluid chlorides for the 24 sites representing sediments from a variety of oceanic environments (references in Table 3). Chlorides are systematically ^{37}Cl-depleted ($\delta^{37}Cl < 0$ ‰) compared to seawater. They form a chlorine reservoir with weighted average $\delta^{37}Cl$ at -2.3 ± 0.2 ‰ and chlorinity at 0.290 ± 0.055 mole Cl^-/kg of sediment or 0.552 ± 0.070 mole Cl^-/kg of pore fluid, assuming that the investigated sites (n = 24) represent a good sampling of the population of the oceanic crustal sediments in terms of diversity and statistical weight. In that case the pore fluid reservoir would be ≈ 1.8 10^8 ± 0.5 km^3 of pore fluid in the oceanic sediments (≈ 3.4 10^8 km^3 of sediment, Straume et al., 2019). This amount of pore fluids is calculated using an average compaction law of $\Phi(z) \approx 0.80 * \exp(-z/1000)$ obtained from the data compiled by Perrier and Quiblier (1974). Of course, this evaluation of the volume of fluid is affected by a great uncertainty, about ± 25%, but this approach allows to obtain a good order of magnitude of this volume to compare it with that of the sea water. Using the pore fluids chlorinity at 0.552 mole $Cl.kg^{-1}$, we deduce that pore fluids would contain 1 10^{20} moles of chloride (= $\sum Q_{porefluid}$), that is about one tenth (13 % exactly) of the chlorides contained in seawater (7.6 10^{20} moles of chloride).

We also provide estimates of the fluxes of expelled chloride from sediment to seawater. They range from 3.5 to 45.6 moles of chloride per square metre per kiloyear (mole $Cl.m^{-2}.ky^{-1}$) (Figure 7). Most of the flux data are in the range between 3 and 25 mole $Cl.m^{-2}.kyr^{-1}$. The mean

601 value is 18.3 mole $Cl.m^{-2}.kyr^{-1}$. These fluxes are very important in terms of controlling the
602 composition of seawater.

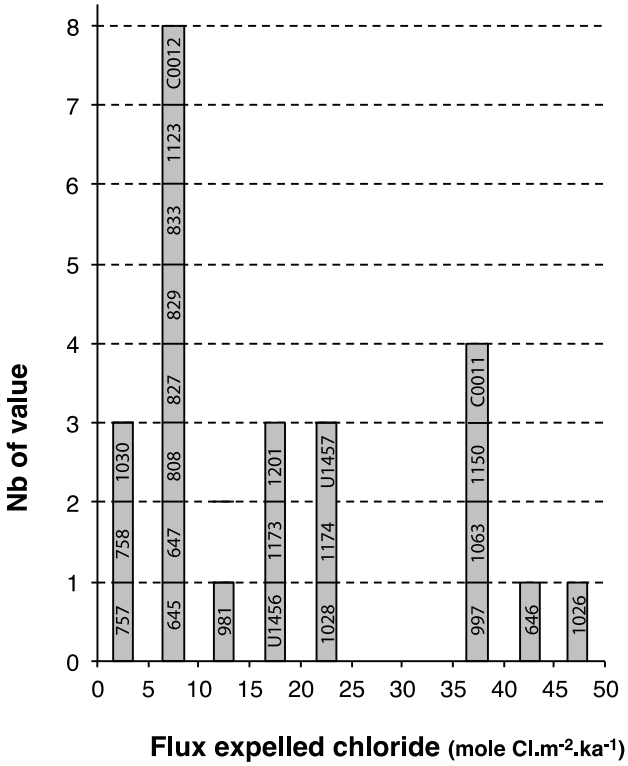

603

604 ***Figure 7:*** *Histogram of expelled chloride flux from the sediments to seawater versus the*
605 *sedimentation rate for 24 sites drilled by IODP. Mean flux value is 14 mole* $Cl.m^{-2}.kyr^{-1}$.
606

607 Using the amount of chloride in the pore fluids of the oceanic sediments and the flux of
608 chloride expelled through the surface of the seafloor (0.14 to 1.8 10^{16} moles of chloride.kyr^{-1} =
609 3.5 to 45.6 mole $Cl.m^{-2}.kyr^{-1}$ * 4 10^{14} m^2), we estimate the equilibration time of chloride
610 between the seawater and the pore fluids of the oceanic sediments:

611

$$\tau_{Cl} = \frac{\sum Q_{Cl\ porefluid}}{Flux_{expelled\ chloride} . surface} \qquad (21)$$

612

it ranges from 5.5 to 71 Myr. The mean value is ≈ 14 Myr. Although small, it is of the same order of magnitude as the mean age of oceanic crust (64.2 Myr; Seton, 2020) and the residence time of chloride in seawater calculated from the chloride river flux (65 Myr; Lecuyer, 2016)

On this timescale, the process fractionating chlorine isotopes in sediments, possibly ion filtration by clays, controls the chloride isotopic contrast between pore fluids and seawater. In this case, an increase of the content of smectites, which are associated with large chlorine isotope fractionation of chlorides, in the sediment would produce more ^{37}Cl-depleted pore fluids and consequently induces an increase in the δ^{37}Cl of seawater chlorides.

Other clays, such as kaolinite, chlorite and illite, which are associated with smaller chlorine isotope fractionation of chlorides, would produce less ^{37}Cl-depleted pore fluids and a smaller increase in the δ^{37}Cl of seawater chlorides. By writing a balance equation (20), one can obtain a model (equation 21) that describes the control of the seawater δ^{37}Cl as a function of chloride partitioning between the seawater and the sediment pore fluids:

$$Q_{\sum Cl}\ \delta^{37}Cl_{\sum Cl} = Q_{Cl\ porefluid}\ \delta^{37}Cl_{porefluid} + Q_{Cl\ seawater}\ \delta^{37}Cl_{Cl\ seawater} \qquad (22)$$

with $Q_{\sum Cl} = Q_{Cl\ porefluid} + Q_{Cl\ seawater}$

we get :

$$\delta^{37}Cl_{Cl\ seawater} = \left(\frac{Q_{Cl\ porefluid}}{Q_{Cl\ seawater}} + 1\right)\ \delta^{37}Cl_{\sum Cl} - \frac{Q_{Cl\ porefluid}}{Q_{Cl\ seawater}}\ \delta^{37}Cl_{porefluid} \qquad (23)$$

Assuming that i) the amounts of Cl in the pore fluid ($Q_{Clporefluid}$) and in the seawater reservoir ($Q_{Clseawater}$) remain constant and ii) the $\delta^{37}Cl_{\sum}$ remains constant, equation 23 shows a linear dependence between $\delta^{37}Cl_{seawater}$ and $\delta^{37}Cl_{porefluid}$ (Figure 8). The second term of equation 23

637 gives the sensitivity of the $\delta^{37}Cl_{seawater}$ response to the isotopic fractionation of chlorine
638 between the pore fluids and the seawater. The sensitivity is weak because it depends on the
639 ratio $Q_{Clporefluid}/Q_{Clseawater}$ (= 0.13) which is small (current values are $Q_{Cl\ pore\ fluid}$ = 1 10^{20} moles of
640 Cl, $Q_{Cl\ seawater}$ = 7.6 10^{20} moles of Cl, $\delta^{37}Cl_{seawater}$ = 0.0 ‰, $\delta^{37}Cl_{pore\ fluids}$ = -2.3 ‰). A first extreme
641 case is when there is no chlorine isotope fractionation of chloride, $\delta^{37}Cl_{seawater}$ and $\delta^{37}Cl_{pore\ fluids}$
642 would be equal to -0.27 ‰. This would be the case if the sediments consisted mainly of
643 carbonates, silica, i.e. minerals that do not fractionate chlorine isotopes from chlorides in the
644 pore fluids. The other extreme is when the fractionation of chlorine isotopes of chloride is
645 maximal. This would be the case if the sediments consisted mainly of smectites, i.e. minerals
646 that fractionate a lot of chlorine isotopes of chlorides. From the available data (Table 2), this
647 condition seems to occur at Sites 1174, C0011 and C0012 where the lowest $\delta^{37}Cl_{porefluids}$ are
648 measured (-4.7, -5.1 and -4.3 ‰ respectively). $\delta^{37}Cl_{seawater}$ would increase to ≈ + 0.25 ‰. The
649 range of variation of $\delta^{37}Cl_{seawater}$ predicted by this chloride partitioning model is between +0.3
650 and -0.3 ‰. It is consistent with the range of variations of $\delta^{37}Cl_{seawater}$ reconstructed from halite
651 deposits for the last 800 million years by Eggenkamp et al. (2019).
652 Then, the clays (content and nature) of the oceanic sediments would play a role in controlling
653 the chlorine isotope composition of chloride of seawater and pore fluids. Since most of the clay
654 minerals present in oceanic sediments, probably more than 90%, are detrital, physically eroded
655 from continental soils (Hillier, 1995 ; Petschick et al., 1996; Thiry, 2000; Fagel, 2007), the
656 nature of clays in oceanic sediments is controlled by the transport of continental clays to the
657 oceans and the alteration style of continental bedrocks. Both are controlled by climatic
658 parameters (precipitation and temperature). This may illustrate a link between the $\delta^{37}Cl$ of
659 seawater and the Earth's climate. If kaolinite is mainly transported to the oceans, the $\delta^{37}Cl$ of
660 seawater would increase slightly. If smectite is mainly transported to the oceans, the $\delta^{37}Cl$ of
661 seawater would increase more (Figure 8).

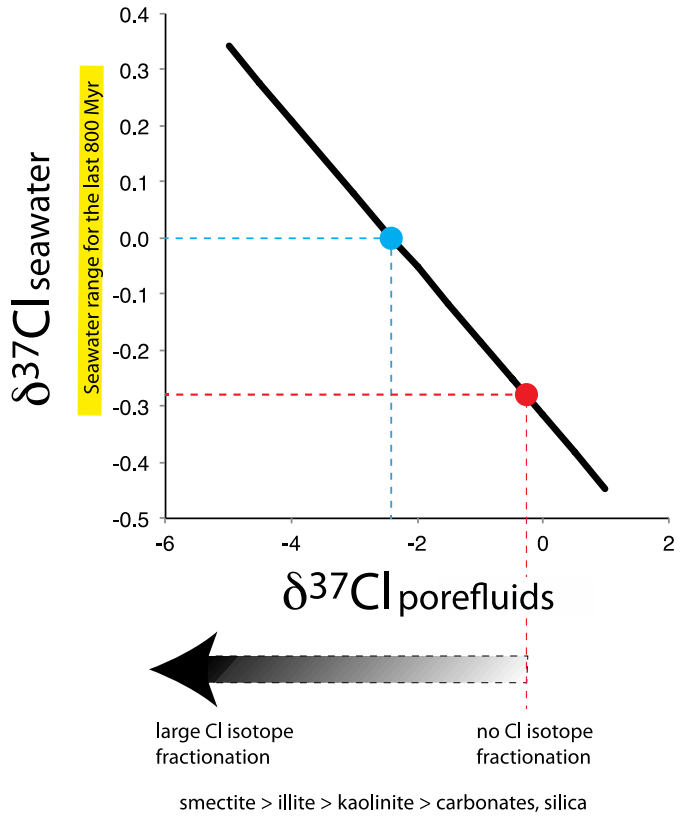

Figure 8: *Relationship between the chlorine isotope composition of seawater ($\delta^{37}Cl_{seawater}$) and the mean chlorine isotope composition of pore fluids of the oceanic sediments ($\delta^{37}Cl_{porefluid}$). Today's compositions is represented with the blue dot, with seawater $\delta^{37}Cl_{seawater}$ = 0 ‰ and mean pore fluid $\delta^{37}Cl_{pore\ fluids}$= -2.3 ‰ (resulting from the chlorine isotope fractionation of chlorides in the sediment induced by ion filtration). In the case where no chlorine isotope fractionation of chlorides due to low abundances of clay minerals and dominance of carbonates and silica in the sediments, the chlorine isotope composition of seawater and that of pore fluids are the same ($\delta^{37}Cl_{seawater}$ = $\delta^{37}Cl_{pore\ fluids}$, = -0.27 ‰, red dot). An increase of the abundance of smectite in the sediment would increase the chlorine isotope fractionation of chlorides by ion filtration resulting in a large ^{37}Cl depletion of the pore fluids and an increase in the $\delta^{37}Cl_{seawater}$. The yellow vertical bar indicates the range of possible $\delta^{37}Cl$ variations of the seawater over the last 800 Myr as determined by Eggenkamp et al. (2019) from halite deposits.*

VI) Conclusions

Chlorine isotope ratios of chlorides in pore fluids from globally distributed clay-rich oceanic sedimentary sites (n=24) show a progressive depletion of ^{37}Cl in chlorides with depth. Mean value for $\delta^{37}Cl$ is -2.3 ± 0.2 ‰ and chlorinity is 0.290 ± 0.055 mole Cl^-/kg of sediment. Assuming that the pore fluids were originally seawater trapped at the seawater-sediment interface, the balance of chlorine isotopes in the pore fluids forces the disappearance of ^{37}Cl-

682 enriched chlorides and since chlorides are the dominant ions in these fluids, this loss of ^{37}Cl-
683 enriched chlorides reveals a very important process operating in the sediment. This process
684 seems independent of the tectonic environment in which the sediments were deposited and
685 amplified by the presence of clays in the sediments.

686 The chlorine budget in these sediments shows that the dominant reservoir of chlorine is the
687 pore fluid chlorides. The other chlorine reservoirs (carbonates, clays, organochlorides) are very
688 modest. Consequently, they do not have the capacity to store the ^{37}Cl-enriched chlorides that
689 the fluids have lost. A review of all the processes that are known to cause a decrease in the δ^{37}Cl
690 of chlorides either by fractionation of chlorine isotopes in chlorides (diffusion, gravity,
691 filtration) or by mixing (advection of ^{37}Cl-depleted chlorides) leaves ion filtration of pore fluid
692 chlorides by clay membranes during the compaction of the sediments as the only known
693 process to date that could explain the widespread ^{37}Cl-depletion in sedimentary pore fluids.

694 The chloride fluxes expelled out of the pore fluids into the seawater calculated here required
695 to explain the observed ^{37}Cl depletions range from 3.5 to 46 moles of chlorides per square
696 metre per kiloyear. Most of the values are between 1 and 25 mole $Cl.m^{-2}.kyr^{-1}$ suggesting that
697 pore fluids and seawater exchange chlorides on the 5.5 to 71 Myr time scale (mean value at ≈
698 14 Myr). At this time scale, the δ^{37}Cl of seawater would be controlled by the nature of the
699 continental detrital clays that are deposited on the seafloor. Minerals with high surface charge
700 density, such as smectites, which are associated with strongly ^{37}Cl-depleted pore-fluids in the
701 sediments, greatly increase the δ^{37}Cl of seawater, whereas minerals with low surface charge
702 density, such as kaolinites, illites-chlorites, which are associated with weakly ^{37}Cl-depleted
703 pore-fluids in the sediments, slightly increase the δ^{37}Cl of seawater. The range of $\delta^{37}Cl_{seawater}$
704 variations must be within -0.3 to +0.3 ‰.

705

706 **VII) Acknowledgement**

We are indebted to the shipboard and drilling personnel, and the Scientific Parties of drillship R/V *JOIDES Resolution* for their dedication and assistance with all aspects of coring, sampling, describing and shipboard laboratory measurements during the Ocean Discovery Program (IODP) Expeditions 355. All the pore fluid samples and most of the data used in this study were acquired during this leg. Additional pore fluids were obtained from the Bremen Core Repository (Holger Kuhlmann) and the Kochi Core Center (Lallan Gupta, Kazuhiro Yoshida, Yusuke Kubo).

Data acquired by the Ocean Drilling Program (ODP), the Integrated Ocean Drilling Program (IODP) and the International Ocean Discovery Program (IODP) and many scientific parties (Legs 105, 131, 134, 162, 164, 168, 172, 181, 186, 190, 195, 322 and 333) were also used in this work. We wish to thank Mark Kendrick, the two anonymous referees for useful criticisms and Benjamin Tutolo that helped us improve the paper. The Comité IODP-France and the TelluS (Syster) Program of CNRS/INSU supported this project.

VIII) Reference

Agrinier P., Destrigneville C., Giunta T., Bonfacie M., Bardoux G., Andre J. and Lucazeau F. (2019) Strong impact of ion filtration on the isotopic composition of chlorine in young clay-rich oceanic sediment pore fluids. Geochim. Cosmochim. Acta 245, 525–541.

Agrinier P., Bonfacie M., Bardoux G., Lucazeau F., Giunta T. and Ader M. (2021) Chlorine isotope data of chlorides challenge the pore fluid paradigm. Geochim. Cosmochim. Acta 300, 258-278.

Andò S, Aharonovich S, Hahn A, George SC, Clift PD, and Garzanti E. (2020) Integrating heavy-mineral, geochemical and biomarker analyses of Plio-Pleistocene sandy and silty turbidites: a novel approach for provenance studies (Indus Fan, IODP Expedition 355). Geological Magazine, 157, 929-938

Balan E., Creon L., Sanloup C., Aleon J., Blanchard M., Paulatto L. and Bureau H. (2019) First-principles modeling of chlorine isotope fractionation between chloride bearing molecules and minerals. Chem. Geol. 525, 424–434.

Barnes J.D., Sharp Z.D. and Fischer T.P. (2008) Chlorine isotope variations across the Izu-Bonin-Mariana arc. Geology,366, 883-886.

Barnes J.D., Sharp Z.D., Fischer T.P., Hilton D.R. and Carr M.J. (2009) Chlorine isotope variations along the Central American volcanic front and back arc. Geochem. Geophys. Geosyst., 10:Q11S17

Berner R.A. (1980) Early Diagenesis: A Theoretical Approach. Princeton Univ. Press.

Boudreau B.P. (1997) Diagenetic Models and Their Implementation, Modelling Transport and Reactions in Aquatic Sediments. 417p. Springer-Verlag. ISBN 3-540-61125-8.

Bonifacie, M., J.L. Charlou, N. Jendrzejewski, P. Agrinier, J.P. Donval. Chlorine isotopic compositions of high temperature hydrothermal vent fluids over ridge axes Chem. Geology, 221 (2005); 279-288.

Bonifacie M., Monnin C., Jendrzejewski N., Agrinier P. and Javoy M. (2007). Chlorine stable isotopic composition of basement fluids of the eastern flank of the Juan de Fuca Ridge (ODP Leg168). Earth Planet. Sci. Lett. 260, 10–22.

Bonifacie, M., N. Jendrzejewski, P. Agrinier, E. Humler, M. Coleman, M. Javoy, (2008a) The chlorine isotope composition of the Earth's mantle, Science, Vol. 319. no. 5869, 1518 - 1520.

Bonifacie, M., V. Busigny, P. Philippot, C. Mével, P. Agrinier, M. Scambelluri, N. Jendrzejewski, M. Javoy (2008b) Chlorine isotopic composition in seafloor peridotites and high-pressure metaperidotites: insights into the oceanic serpentinization and subduction processes, Geochim. Cosmochim. Acta, *72, 1*, 126-139.

Cai M, Xu Z, Clift PD, Khim B-K, Lim D, Yu Z, Kulhanek DK, and Li T. (2020). Long-term history of sediment inputs to the eastern Arabian Sea and its implications for the evolution of the Indian summer monsoon since 3.7 Ma. Geological Magazine, 157, 908-919.

Carter, S.C., Griffith, E.M., Scher, H.D., and the Expedition 355 Scientists (2017). Data report: 87Sr/86Sr in pore fluids from IODP Expedition 355 Arabian Sea Monsoon. *In* Pandey, D.K., Clift, P.D., Kulhanek, D.K., and the Expedition 355 Scientists, *Arabian Sea Monsoon*. Proceedings of the International Ocean Discovery Program, 355: College Station, TX (International Ocean Discovery Program).

Carter SC, Griffith EM, Clift PD, Scher HD, and Dellapenna TM. (2020). Clay-fraction strontium and neodymium isotopes in the Indus Fan: implications for sediment transport and provenance. Geological Magazine, 157, 879-894

Carter, R.M., McCave, I.N., Richter, C., Carter, L., et al. (1999) *Proc. ODP, Init. Repts.*, 181 : College Station, TX (Ocean Drilling Program), Shipboard Scientific Party. Site 1123: North Chatham Drif a 20-Ma Record of the Pacific Deep Western Boundary Current, 1-184.

Clift P.D., Kulhanek D.K., Zhou P., Bowen M.G., Vincent S.M., Lyle M. and Hahn A. (2020). Chemical weathering and erosion responses to changing monsoon climate in the Late Miocene of Southwest Asia. Geological Magazine, 157, 939-955.

Chen H., Xu Z., Clift P.D., Lim D., Khim B.-K., Yu Z. (2019). Orbital-scale evolution of the Indian summer monsoon since 1.2 Ma: Evidence from clay mineral records at IODP Expedition 355 Site U1456 in the eastern Arabian Sea. Journal of Asian Earth Sciences 174, 11–22.

Chen, H., Xu, Z., Lim, D., Clift, P. D., Chang, F., Li, T., Cai1, M., , W. , Yu, Z, and Sun R. (2020). Geochemical records of the provenance and silicate weathering/erosion from the eastern Arabian Sea and their responses to the Indian summer monsoon since the Mid**-**Pleistocene. Paleoceanography and Paleoclimatology, 35, e2019PA003732.

Coleman M.L., Eggenkamp H.G.M. and Aranyossy, J.-F. (2001). Chlorine stable isotope characterisation of solute transport in mudrocks. ANDRA: Actes des journées scientifiques 1999. Chapter 10, 155-175, EDP Sciences, France.

Collot, J.-Y., Greene, H.G., Stokking, L.B., et al., (1992a) *Proc. ODP, Init. Repts.*, 134: College Station, TX (Ocean Drilling Program), Shipboard Scientific Party, 1992. Site 827 95–137.

Collot, J.-Y., Greene, H.G., Stokking, L.B., et al., (1992b) *Proc. ODP, Init. Repts.*, 134: College Station, TX (Ocean Drilling Program), Shipboard Scientific Party, 1992. Site 829 179–260.

Collot, J.-Y., Greene, H.G., Stokking, L.B., et al., (1992c) *Proc. ODP, Init. Repts.*, 134: College Station, TX (Ocean Drilling Program), Shipboard Scientific Party, 1992. Site 833 479–557.

Davis E. E., Fisher A. T. and Firth J. V., et al. (1997a) *Proc. ODP, Init. Repts.*, 168: College Station, TX (Ocean Drilling Program), Shipboard Scientific Party. Rough basement transect (Sites 1026 and 1027). 101-160.

Davis E. E., Fisher A. T. and Firth J. V., et al. (1997b) *Proc. ODP, Init. Repts.*, 168: College Station, TX (Ocean Drilling Program), Shipboard Scientific Party. Buried basement transect (Sites 1028, 1029, 1030, 1031, and 1032). 161-212.

Deyhle A., Kopf A., Frape S. and Hesse R. (2003) Evidence for fluid flow in the Japan Trench forearc using isotope geochemistry (Cl, Sr, B): Results from ODP Site 1150. The Island Arc **13**, 258–270.

Desaulniers, D.E., Kaufmann, R.S., Cherry, J.A., Bentley, H.W. (1986). ^{37}Cl–^{35}Cl variations in a diffusion-controlled groundwater system. Geochim. Cosmochim. Acta 50, 1757–1764.

Eggenkamp H.G.M. (1994). $\delta^{37}Cl$: The Geochemistry of Chlorine Isotopes. Ph.D. Thesis. Utrecht University, Utrecht.

Eggenkamp H.G.M. and Coleman M. L. (2009). The effect of aqueous diffusion on the fractionation of chlorine and bromine stable isotopes. Geochim. Cosmochim. Acta 73, 3539–3548.

Eggenkamp H., Bonifacie M., Ader M., Agrinier P. (2016) Experimental determination of stable chlorine and bromine isotope fractionation during precipitation of salt from a saturated solution. Chemical Geology 433, 46-56.

Eggenkamp H.G.M., Louvat P., Agrinier P., Bonifacie M., Bekker A., Krupenik V., Griffioen J., Horita J., Brocks J.J., Bagheri R. (2019) The bromine and chlorine isotope composition of primary halite deposits and their significance for the secular isotope composition of seawater. Geochim. Cosmochim. Acta 264, 13-29.

Eggenkamp H.G.M., Marks M.A.W., Bonifacie M., Bardoux G., Agrinier P. and Markl G. (2022) Cl isotope fractionation in magmatic and hydrothermal eudialyte, sodalite and tugtupite (Ilímaussaq intrusion, South Greenland). Chemical Geology, 604, 1-12.

Fagel N. (2007). Clay Minerals, Deep Circulation and Climate. Developments in Marine Geology, Volume 1, 139-184

Gieskes, J.M., Lawrence, J.R. (1976). Interstitial water studies, Leg 35. Initial Rep. DSDP. 35, 407–424.

Gieskes, J.M., Gamo, T., and Brumsack, H. (1991). *Technical Note 15: Chemical Methods for Interstitial Water Analysis Aboard JOIDES Resolution.* Ocean Drilling Program.

Giunta T., Devauchelle O., Ader M., Locke R., Louvat P., Bonifacie M., Métivier F. and Agrinier P. (2017a). The gravitas of gravitational isotope fractionation revealed in an isolated aquifer. Geochem. Perspect. Lett. 4, 53–58.

Giunta T., Labidi J. and Eggenkamp H. G. M. (2017b). Chlorine isotope fractionation between chloride (Cl^-) and dichlorine (Cl_2). Geochim. Cosmochim. Acta 213, 375–382.

Godon A., Jendrzejewski N., Castrec-Rouelle M., Dia A., Pineau F., Boulègue J. and Javoy M. (2004a). Origin and evolution of fluids from mud volcanoes in the Barbados accretionary complex. Geochim. Cosmochim. Acta **68**, 2153–2165.

Godon A., Jendrzejewski N., Eggenkamp H. G. M., Banks D. A., Ader M., Coleman M. L. and Pineau F. (2004b) A cross calibration of chlorine isotopic measurements and suitability of seawater as the international reference material. Chem. Geol., 207, 1–12.

Henry P., Kanamatsu T., Moe K.T., Strasser M. and the Expedition 333 Scientists (2012) Proc. IODP, 333. Integrated Ocean Drilling Program Management International, Inc., Tokyo. Scientific Drilling, 14, 4–17.

Hesse R., Frape S.K., Egeberg P.K. and Matsumoto R. (2000). Stable isotope studies (Cl, O, and H) of interstitial waters from Site 997, Black ridge gas hydrate field, West Atlantic. Proc. ODP, Sci. Results 164, 129–137.

Hesse R., Egeberg P.K. and Frape S.K. (2006). Chlorine stable isotope ratios as tracer for pore-water advection rates in a submarine gas-hydrate field: implication for hydrate concentration. Geofluids, 6, 1-7.

Hillier S. (1995) Erosion, sedimentation and sedimentary origin of clays. p162-219 in Origin and Mineralogy of Clays (B. Velde, editor). Springer, Berlin

Hutchison I. (1985). The effects of sedimentation and compaction on oceanic heat flow. Geophys. J. R. Astr. Soc. 82, 439–459.

Jansen, E., Raymo, M.E., Blum, P., et al., (1996) *Proc. ODP, Init. Repts.*, 162: College Station, TX (Ocean Drilling Program), Shipboard Scientific Part. Sites 980/981 49–90.

Kaufmann R.S., Long A., Bentley H. and Davis S. (1984). Natural chlorine isotope variations. Nature, 309, 339-340

Keigwin, L.D., Rio, D., Acton, G.D., et al., (1998) *Proc. ODP, Init. Repts.*, 172: College Station, TX (Ocean Drilling Program), Shipboard Scientific Part. Bermuda Rise and Sohm Abyssal Plain, Sites 1063 and 1064, 253-310.

Kendrick, M.A. (2018). Halogens in seawater, marine sediments and the altered oceanic lithosphere. In: Harlov, D.E., Aranovich, L. (Eds.), The Role of Halogens in Terrestrial and Extraterrestrial Geochemical Processes, Springer Geochemistry, pp. 591–648. (chapter 9).

Khim B-K, Horikawa K, Asahara Y, Kim J., and Ikehara M. (2018). Detrital Sr–Nd isotopes, sediment provenances and depositional processes in the Laxmi Basin of the Arabian Sea during the last 800 ka. Geological Magazine, 157-6, 895-907.

Kumar A, Dutt S, Saraswat R, Gupta AK, Clift PD, Pandey DK, Yu Z, and Kulhanek DK. (2019). A late Pleistocene sedimentation in the Indus Fan, Arabian Sea, IODP Site U1457. Geological Magazine, 157-6, 1001-1011.

Lavastre V., Jendrzejewski N., Agrinier P., Javoy M. and Evrard M. (2005). Chlorine transfer out of a very low permeability clay sequence (Paris basin, France): 35Cl and 37Cl evidence. Geochim. Cosmochim. Acta 69, 4949–4961.

Lecuyer C. (2016). Seawater residence times of some elements of geochemical interest and the salinity of the oceans. Bull. Soc. géol. France, 187, 6, 245-260.

Lawrence J. R., Gieskes J. M. and Broecker W. S. (1975). Oxygen isotope and cation composition of DSDP pore waters and the alteration of layer II basalts. Earth Planet. Sci. Lett. 27, 1–10.

Li L., Bonifacie M., Aubaud C., Crispi O., Dessert C. and Agrinier P. (2015) Chlorine isotopes of thermal springs in arc volcanoes for tracing shallow magmatic activity. Earth Planet. Sci. Lett. 413, 101–110.

Liu X., Wei H.-Z., Li Y.-C., Williams-Jones A.E., Lu J.-J., Jiang S.-Y., Dong G., Ma J., Eastoe C.J. (2021). Chlorine isotope mantle heterogeneity: Constraints from theoretical first-principles calculations. Chemical Geology, 572, 1-14.

Lucazeau F. and Le Douaran S. (1985) The blanketing effect of sediments in basins formed by extension: a numerical model. Application to the Gulf of Lion and Viking graben. Earth and Planetary Science Letters, 74, 92-102.

Manheim, F. T, (1966). A hydraulic squeezer for obtaining interstitial water from consolidated and unconsolidated sediments. U.S. Geol. Surv. Prof. Paper 550-C, 256-261.

Murray, R.W., Miller, D.J., and Kryc, K.A. (2000). Technical Note 29: Analysis of Major and Trace Elements in Rocks, Sediments, and Interstitial Waters by Inductively Coupled Plasma–Atomic Emission Spectrometry (ICP-AES). Ocean Drilling Program.

Mazurek M., Oyama T., Wersin T. and Alt-Epping P. (2015). Pore-water squeezing from indurated shales. Chemical Geology **400**, 106–121.

Moore, G.F., Taira, A., Klaus, A., et al. (2001a) *Proc. ODP, Init. Repts.*, 190: College Station, TX (Ocean Drilling Program), Shipboard Scientific Party. Site 1173 1-149.

Moore, G.F., Taira, A., Klaus, A., et al. (2001b) *Proc. ODP, Init. Repts.*, 190: College Station, TX (Ocean Drilling Program), Shipboard Scientific Party. Site 1174 1-147.

Pandey, D.K., Clift, P.D., Kulhanek, D.K., Andò, S., Bendle, J.A.P., Bratenkov, S., Griffith, E.M., Gurumurthy, G.P., Hahn, A., Iwai, M., Khim, B.-K., Kumar, A., Kumar, A.G., Liddy, H.M., Lu, H., Lyle, M.W., Mishra, R., Radhakrishna, T., Routledge, C.M., Saraswat, R., Saxena, R., Scardia, G., Sharma, G.K., Singh, A.D., Steinke, S., Suzuki, K., Tauxe, L., Tiwari, M., Xu, Z., and Yu, Z., (2016a). Expedition 355 summary. *In* Pandey, D.K., Clift, P.D., Kulhanek, D.K., and the Expedition 355 Scientists, *Arabian Sea Monsoon.* Proceedings of the International Ocean Discovery Pro- gram, 355: College Station, TX (International Ocean Discovery Program).

Pandey, D.K., Clift, P.D., Kulhanek, D.K., Andò, S., Bendle, J.A.P., Bratenkov, S., Griffith, E.M., Gurumurthy, G.P., Hahn, A., Iwai, M., Khim, B.-K., Kumar, A., Kumar, A.G., Liddy, H.M., Lu, H., Lyle, M.W., Mishra, R., Radhakrishna, T., Routledge, C.M., Saraswat, R., Saxena, R., Scardia, G., Sharma, G.K., Singh, A.D., Steinke, S., Suzuki, K., Tauxe, L., Tiwari, M., Xu, Z., and Yu, Z., (2016b). Site U1456. *In* Pandey, D.K., Clift, P.D., Kulhanek, D.K., and the Expedition 355 Scientists, *Arabian Sea Monsoon.* Proceedings of the International Ocean Discovery Program, 355: College Station, TX (International Ocean Discovery Program).

Pandey, D.K., Clift, P.D., Kulhanek, D.K., Andò, S., Bendle, J.A.P., Bratenkov, S., Griffith, E.M., Gurumurthy, G.P., Hahn, A., Iwai, M., Khim, B.-K., Kumar, A., Kumar, A.G., Liddy, H.M., Lu, H., Lyle, M.W., Mishra, R., Radhakrishna, T., Routledge, C.M., Saraswat, R., Saxena, R., Scardia, G., Sharma, G.K., Singh, A.D., Steinke, S., Suzuki, K., Tauxe, L., Tiwari, M., Xu, Z., and Yu, Z., (2016c). Site U1457. In Pandey, D.K., Clift, P.D., Kulhanek, D.K., and the Expedition 355 Scientists, Arabian Sea Monsoon. Proceedings of the International Ocean Discovery Program, 355: College Station, TX (International Ocean Discovery Program).

Pandey, D.K., Clift, P.D., Kulhanek, D.K., Andò, S., Bendle, J.A.P., Bratenkov, S., Griffith, E.M., Gurumurthy, G.P., Hahn, A., Iwai, M., Khim, B.-K., Kumar, A., Kumar, A.G., Liddy, H.M., Lu, H., Lyle, M.W., Mishra, R., Radhakrishna, T., Routledge, C.M., Saraswat, R., Saxena, R., Scardia, G., Sharma, G.K., Singh, A.D., Steinke, S., Suzuki, K., Tauxe, L., Tiwari, M., Xu, Z., and Yu, Z., (2016d). Expedition 355 methods. *In* Pandey, D.K., Clift, P.D., Kulhanek, D.K., and the Expedition 355 Scientists, *Arabian Sea Monsoon.* Proceedings of the International Ocean Discovery Pro- gram, 355: College Station, TX (International Ocean Discovery Program).

Paull, C.K., Matsumoto, R., Wallace, P.J., et al., (1996) Proc. ODP, Init. Repts., 164: College Station, TX (Ocean Drilling Program), Shipboard Scientific Party, 1996. Site 997 277–334.

Perrier R. and Quiblier J. (1974) Thickness Changes in Sedimentary Layers During Compaction History; Methods for Quantitative Evaluation. The American Association of Petroleum Geologists Bulletin 58-3, 507-520.

Peirce, J., Weissel, J., et al., (1989a) *Proc. ODP, Init. Repts.*, 121: College Station, TX (Ocean Drilling Program), Shipboard Scientific Party. Site 757 305–358.

Peirce, J., Weissel, J., et al., (1989b) *Proc. ODP, Init. Repts.*, 121: College Station, TX (Ocean Drilling Program), Shipboard Scientific Party. Site 758 359–453.

Petschick R., Kuhn G. and Gingele F. (1996). Clay Minerals in surface sediments of the South Atlantic: Sources, transport and relation to oceanography. Marine Geology, 130, 203-229.

Phillips F. M. and Bentley H. W. (1987). Isotopic fractionation during ion filtration: I. theory. Geochim. Cosmochim. Acta 51, 683–695.

Ransom B., Spivack A. J. and Kastner M. (1995). Stable Cl isotopes in subduction-zone pore waters: Implications for fluid-rock reactions and the cycling of chlorine. Geology 23, 715–718.

Richard A., Banks D.A., Mercadier J., Boiron M.-C., Cuney M. and Cathelineau M., (2011). An evaporated seawater origin for the ore-forming brines in unconformity-related uranium deposits (Athabasca Basin, Canada): Cl/Br and δ^{37}Cl analysis of fluid inclusions. Geochim. Cosmochim. Acta **75**, 2792-2810.

Richet, P., Bottinga, Y., Javoy, M. (1977). A review of hydrogen, carbon, nitrogen, oxygen, and chlorine stable isotope fractionation among gaseous molecules. Annu. Rev. Earth Planet. Sci. 5, 65–110.

Routledge CM, Kulhanek DK, Tauxe L, Scardia G, Singh AD, Steinke S, Griffith EM, and Saraswat R. (2020). A revised chronostratigraphic framework for International Ocean Discovery Program Expedition 355 sites in Laxmi Basin, eastern Arabian Sea. Geological Magazine, 157, 961-978.

Taira, A., Hill, I., Firth, J.V., et al., (1991) *Proc. ODP, Init. Repts.*, 131: College Station, TX (Ocean Drilling Program), Shipboard Scientific Party, 1991. Site 808 71–269.

Thiry M. (2000) Palaeoclimatic interpretation of clay minerals in marine deposits: an outlook from the continental origin. Earth-Science Reviews 49, 201–221

Sacks, I.S., Suyehiro, K., Acton, G.D., et al., (2000) *Proc. ODP, Init. Repts.*, 186: College Station, TX (Ocean Drilling Program), Shipboard Scientific Party, 1992. Site 1150 1-208.

Saito S. & the Expedition 322 Scientists (2010a). Site C0011. In Proc. IODP, 322 (eds. S. Saito, M. B. Underwood and Y. Kubo), and the Expedition 322 Scientists. Integrated Ocean Drilling Program Management International, Inc., Tokyo.

Saito S. & the Expedition 322 Scientists (2010b). Site C0012. In Proc. IODP, 322 (eds. S. Saito, M. B. Underwood and Y. Kubo), and the Expedition 322 Scientists. Integrated Ocean Drilling Program Management International, Inc., Tokyo.

Salisbury, M.H., Shinohara, M., Richter, C., et al. (2002) Proc. ODP, Init. Repts., 195: College Station, TX (Ocean Drilling Program), Shipboard Scientific Party. Site 1201 1-233.

Schauble, E.A., Rossman, G.R., Taylor, H.P. (2003). Theoretical estimates of equilibrium chlorine-isotope fractionations. Geochim. Cosmochim. Acta 67, 3267–3281.

Seton, M., Müller, R. D., Zahirovic, S., Williams, S., Wright, N. M., Cannon, J., et al. (2020). A global data set of present- day oceanic crustal age and seafloor spreading parameters. Geochemistry, Geophysics, Geosystems, 21, e2020GC009214.

Sharp Z., Barnes J.D., Fischer T.P., Halick M. (2010). An experimental determination of chlorine isotope fractionation in acid systems and applications to volcanic fumaroles. Geochim. Cosmochim. Acta 74, 264–273

Straume, E. O., Gaina, C., Medvedev, S., Hochmuth, K., Gohl, K., Whittaker, J. M., et al. (2019). GlobSed: Updated total sediment thickness in the world's oceans. Geochemistry, Geophysics, Geosystems, 20, 1756–1772.

Spivack A. J., Kastner M. and Ransom B. (2002). Elemental and isotopic chloride geochemistry and fluid flow in the Nankai trough. Geophys. Res. Lett. **29**, 1661–1665.

Srivastava, S.P., Arthur, M., Clement, B., et al., (1987a) *Proc. ODP, Init. Repts.*, 105: College Station, TX (Ocean Drilling Program), Shipboard Scientific Party. Site 645. 61–418.

Srivastava, S.P., Arthur, M., Clement, B., et al., (1987b) *Proc. ODP, Init. Repts.*, 105: College Station, TX (Ocean Drilling Program), Shipboard Scientific Party. Site 646. 419–674.
Srivastava, S.P., Arthur, M., Clement, B., et al., (1987c) *Proc. ODP, Init. Repts.*, 105: College Station, TX (Ocean Drilling Program), Shipboard Scientific Party,. Site 647. 675–905.
Urey H.C. (1947) The thermodynamic properties of isotopic subtances. The Journal of the Chemical Society, 562-581.
Wei, W., Kastner, M., Deyhle, A., and Spivack, A.J., (2005). Geochemical cycling of fluorine, chlorine, bromine, and boron and implications for fluidrock reactions in Mariana forearc, South Chamorro Seamount, ODP Leg 195. In Shinohara, M., Salisbury, M.H., and Richter, C. (Eds.), Proc. ODP, Sci. Results, 195, 1–23.
Wei W., Kastner M. and Spivack A. J. (2008). Chlorine stable isotopes and halogen concentrations in convergent margins with implications for the Cl isotopes cycle in the ocean. Earth Planet. Sci. Lett. 266, 90–104.

Table 1 : Chloride concentrations, chlorine isotope composition of chlorides and oxygen isotope composition of water of pore fluids from Sites U1456 and U1457 drilled during Leg 355. Chloride concentrations and porosity values are from Pandey et al. (2016b & c)

355-	Depth	Porosity	[Cl⁻]	$\delta^{37}Cl_{SMOC}$
U1456A-1H-2	2.95	73	556.72	-0.01
U1456A-4H-5	30.95	66	559.60	-0.29
U1456A-7H-5	59.45	64	556.49	-0.46
U1456A-10H-5	87.95	60	555.21	-0.65
U1456A-14H-3	122.95	60	557.07	-0.89
U1456A-19F-2	151.65	48	559.55	-0.98
U1456A-25F-3	180.56	48	560.37	-1.04
U1456A-33F-2	216.65	45	564.80	-1.11
U1456A-38F-2	238.65	49	560.75	-1.12
U1456A-42F-2	256.91	47	559.36	-1.17
U1456A-49F-1	287.55	44	561.67	-1.25
U1456A-63F-1	353.3	46	567.29	-1.46
U1456A-67F-2	373.6	46	562.74	-1.42
U1456A-71X-3	393.9	46	565.58	-1.61
U1456A-73X-5	414.8	42	569.10	-1.62
U1456C-41X-2	430.6	42	568.80	-1.58
U1456C-45X-2	458.41	42	568.66	-1.73
U1456D-7R-1	508.14	44	570.23	-1.54
U1456D-9R-5	533.82	46	564.97	-1.72
U1456D-16R-2	596.99	44	551.16	-1.87
U1456D-20R-1	634.8	44	567.55	-2.25
U1456D-21R-2	645.75	44	569.91	-1.97
U1456D-29R-2	723.18	45	571.57	-2.39
U1456D-31R-1	741.45	41	565.10	-2.50
U1456D-37R-3	802.64	46	572.85	-2.39
U1457A-1H-6	7.9	66	564.40	-0.04
U1457A-3H-5	25.7	64	561.15	-0.19
U1457A-5H-2	40.2	64	559.18	-0.28
U1457A-7H-5	63.6	62	559.21	-0.40
U1457A-9H-5	81.1	49	558.41	-0.44
U1457A-11H-2	97.2	48	560.89	-0.39
U1457B-15F-2	118.3	49	558.15	-0.41
U1457B-23F-2	155.8	48	556.30	-0.42
U1457B-31F-2	193.4	44	554.68	-0.42
U1457C-18R-6	355.7	44	555.55	-0.52
U1457C-22R-3	390	46	556.95	-0.47
U1457C-25R-2	417.5	52	552.37	-0.58
U1457C-34R-2	504.9	43	560.01	-0.64
U1457C-37R-1	532.5	45	562.84	-0.81
U1457C-39R-2	553.4	41	563.71	-0.79
U1457C-41R-2	572.2	43	566.17	-0.75
U1457C-44R-4	604.5	40	560.31	-0.87
U1457C-47R-5	635.5	45	567.03	-0.93
U1457C-51R-4	672.7	39	563.07	-1.20
U1457C-58R-3	738.3	37	568.25	-1.08
U1457C-64R-1	794.4	39		-1.40
U1457C-66R-2	815.0	36	566.56	-1.28

Table 2: Budget of pore fluids and pore fluid chlorides in Sites U1456 and U1457 and 22 other IODP Sites

Site	Present day sedimentary pile											Decompacted sedimentary pile			Fluid in excess (expelled by compaction)					
	Age (Ma)[1]	Thickness (m)[2]	Porosity (min, max)[3]	$[Cl^-]_{extrema}$ ($kM.kg^{-1}$)[4]	$V_{porefluid}$ (m^3)[5]	V_{solid} (m^3)[6]	$Q_{H2O\ porefluid}$ (kM H2O)[7]	$Q_{Cl\ porefluid}$ (kM Cl)[8]	$\delta^{37}Cl_{porefluid}$ (‰)[9]	$[Cl\text{-}]_{porefluid}$ ($M.kg^{-1}$)[10]	$Q_{Cl\ solid}$ (kM Cl)[11]	Thickness (m)[12]	$V_{porefluid}$ (m^3)[13]	$Q_{Cl\ porefluid}$ (kM Cl)[14]	$V_{lost\ porefluid}$ (m^3)[15]	$Q_{Cl\ lost}$ (kM Cl)[16]	$\delta^{37}Cl_{Cl\ loss}$ (‰)[17]	$[Cl\text{-}]_{lost\ fluid}$ ($M.kg^{-1}$)[18]	$Flux_{expelled\ chloride}$ (Mole $Cl.m^{-2}.kyr^{-1}$)[19]	$Flux_{expelled\ fluid}$ (Mole $H_2O.m^{-2}.kyr^{-1}$)[20]
U1456	11	1000	0.80, 0.38	0.572	457	543	25081	252	-1.59	0.571	8.6	1357	814	543	357	187	2.3	0.512	17.0	1783
U1457	10	1000	0.80, 0.38	0.568	454	546	24891	246	-0.73	0.530	8.6	1401	855	546	401	231	0.8	0.562	23.1	2201
645	20	1100	0.55, 0.33	0.603	519	581	28502	294	-3.2	0.553	9.2	1452	871	486	352	192	4.9	0.534	9.6	965
646	8	800	0.74, 0.40	0.571	432	368	23711	241	-2.2	0.545	5.8	1415	1047	584	615	343	1.5	0.545	42.9	4219
647	50	700	0.72, 0.37	0.524	379	321	20783	217	-2.1	0.560	5.1	1285	964	538	585	321	1.4	0.536	6.4	642
757	50	340	0.75, 0.24	0.593	153	187	8372	87	-0.9	0.557	3.0	750	562	314	410	227	0.3	0.541	4.5	450
758	70	520	0.75, 0.32	0.566	261	259	14314	146	-1.2	0.547	4.1	1037	777	434	517	288	0.6	0.544	4.1	405
808	13.6	830	0.62, 0.29	0.460	473	357	25968	282	-5	0.582	5.6	1081	724	404	251	122	11.5	0.475	9.0	1014
827	1.75	240	0.60, 0.40	0.614	129	111	7059	76	-0.4	0.577	1.8	265	154	86	25	10	3.1	0.381	5.6	789
829	3	143	0.65, 0.30	0.565	75	68	4095	42.2	-0.1	0.552	1.1	171	103	57	28	15	0.3	0.526	5.0	511
833	3	494	0.70, 0.40	1.2	234	260	12835	191	-0.4	0.798	4.1	650	390	218	156	27	2.9	0.167	8.9	2859
981	3.5	268	0.70, 0.52	0.57	168	100	9226	88.8	-0.92	0.516	1.6	333	233	130	65	41	2.0	0.621	11.8	1018
997	6	747	0.72, 0.52	0.416	435	312	23884	218	-2.2	0.489	4.9	1113	802	447	366	229	2.1	0.611	38.2	3352
1026	1.5	228	0.70, 0.48	0.577	122	106	6676	70	-0.4	0.562	1.7	354	248	138	126	68	0.4	0.529	45.6	4628
1028	1.25	131	0.75, 0.55	0.572	84	47	4598	48	-0.5	0.560	0.7	189	142	79	58	31	0.8	0.524	24.8	2540
1030	0.65	42	0.72, 0.65	0.568	29	13	1592	16.34	-0.4	0.550	0.2	46	33	19	4	2	2.8	0.511	3.5	372
1063	3.2	394	0.75, 0.50	0.56	244	150	13403	136	-0.9	0.544	2.4	599	449	251	205	115	1.1	0.546	35.8	3517
1123	10	321	0.75, 0.50	0.58	198	123	10849	112	-0.7	0.553	1.9	440	317	177	119	65	1.2	0.531	6.5	655
1150	10	1168	0.73, 0.56	0.3	757	411	41522	321	-0.6	0.414	6.5	1626	1215	678	458	357	0.5	0.761	35.7	2513
1173	13	674	0.70, 0.50	0.5	348	326	19107	190	-3.65	0.533	5.1	1086	760	424	412	234	3.0	0.555	18.0	1739
1174	13	1109	0.62, 0.25	0.47	486	623	26669	266	-5	0.535	9.8	1640	1016	567	531	301	4.4	0.555	23.2	2239
1201	35	505	0.85, 0.40	0.662	270	235	14828	164	-1.1	0.593	3.7	1565	1330	742	1060	578	0.3	0.533	16.5	1662
C0011	14	858	0.72, 0.35	0.51	438	420	24022	241	-5.2	0.538	6.6	1751	1331	743	893	502	2.5	0.549	35.8	3500
C0012	15	340	0.80, 0.30	0.61	196	144	10771	99	-3.8	0.493	2.3	513	370	206	173	107	3.5	0.604	7.1	634

1 : Age of the oldest cored sediment from which pore fluid was extracted;
2: Depth of the oldest cored sediment from which pore fluid was extracted;
3: Porosity maximum and minimum of the sediment;
4: Chlorinity extrema of the pore fluids (maximum if $[Cl^-] > [Cl^-]_{seawater}$ or minimum if $[Cl^-] < [Cl^-]_{seawater}$);
5: Volume of pore fluid (equation 1);
6: Volume of the solid (equation 7);
7: Amount of water in the pore fluids (equation 2);
8: Amount of chloride in the pore fluids (equation 3);
9: Mean $\delta^{37}Cl$ value of the chlorides of the porefluid (equation 4)
10: Mean $[Cl^-]$ value in the pore fluids (equation 5);
11: Amount of chloride in the solid of the sedimentary pile (equation 6);
12: Decompacted thickness of the sedimentary pile (equation 13);
13: Volume of pore fluid in the decompacted pile (equation 14);
14: Amount of chloride in the decompacted pile (equation 17);
15: Volume of lost pore fluid from the decompacted pile (equation 15);
16: Amount of lost chloride from the sediment (equation 16)
17: Mean value of the $\delta^{37}Cl$ of lost porefluid chlorides from the decompacted pile (equation 9);
18: Mean value of the chlorinity of lost porefluid chlorides (equation 19)
19: Mean flux of expelled chloride (equation 19);
20: Mean flux of expelled water (equation 20);
kM: kilo mol

943
944

945 Table 3: References for the 24 oceanic sites drilled by IODP

Site	Leg	Reference for data
U1456	355	Pandey, D.K. et al. (2016b)
U1457	355	Pandey, D.K. et al. (2016c)
645	105	Srivastava S. P., Arthur M. and Clement B., et al. (1987a)
646	105	Srivastava S. P., Arthur M. and Clement B., et al. (1987b)
647	105	Srivastava S. P., Arthur M. and Clement B., et al. (1987c)
757	121	Peirce J. and Weissel J., et al. (1989a)
758	121	Peirce J. and Weissel J., et al. (1989b)
808	131	Taira, A. Hill, I., Firth, J., et al. 1991, Spivack et al. (2002)
827	134	Collot, J.-Y., Greene, H.G., Stokking, L.B., et al. (1992a)
829	134	Collot, J.-Y., Greene, H.G., Stokking, L.B., et al. (1992b)
833	134	Collot, J.-Y., Greene, H.G., Stokking, L.B., et al. (1992c)
981	162	Jansen, E., Raymo, M.E., Blum, P., et al. (1996)
997	164	Paull, C.K., Matsumoto, R., Wallace, P.J., et al. (1996), Hesse et al. (2000)
1026	168	Davis E. E., Fisher A. T. and Firth J. V., et al. (1997a), Bonifacie et al. (2007)
1028	168	Davis E. E., Fisher A. T. and Firth J. V., et al. (1997b), Bonifacie et al. (2007)
1030	168	Davis E. E., Fisher A. T. and Firth J. V., et al. (1997b), Bonifacie et al. (2007)
1063	172	Keigwin, L.D., Rio, D., Acton, G.D., et al., (1998)
1123	181	Carter, R.M., McCave, I.N., Richter, C., Carter, L., et al. (1999)
1150	186	Sacks, I.S., Suyehiro, K., Acton, G.D., et al., (2000), Deyhle A. et al. (2003)
1173	190	Moore, G.F., Taira, A., Klaus, A., et al. (2001a), Wei et al. (2008)
1174	190	Moore, G.F., Taira, A., Klaus, A., et al. (2001b), Wei et al. (2008)
1201	195	Salisbury, M.H., Shinohara, M., Richter, C., et al. (2002)
C0011	322 & 333	Saito, S., et al. (2010a). Henry P. et al. (2012)
C0012	322 & 333	Saito, S., et al. (2010b). Henry P. et al. (2012)

946
947